NASA Contractor Report 175076

Heat Transfer to Two-Phase Air/Water Mixtures Flowing in Small Tubes With Inlet Disequilibrium

J.M. Janssen, L.W. Florschuetz, and J.P. Fiszdon

Arizona State University
Tempe, Arizona

March 1986

Prepared for
Lewis Research Center
Under Grant NSG-3075

National Aeronautics and
Space Administration

CONTENTS

NOMENCLATURE

Variables

a,b - coefficients of correlation equation for tube wall resistance

Cp - isobaric specific heat (J/kg-K)

D - diameter (m)

G - mass flux (kg/s-m^2)

h - heat transfer coefficient (W/m^2-K)

i - specific enthalpy (J/kg)

I - current (A)

K - thermal conductivity (W/m-K)

L - length of test section (m)

M - mass flow rate (kg/s)

n - variable exponent in correlation 3-9

Nu - Nusselt number (hD/K)

P - pressure (Pa)

Pr - Prandtl number ($C_p \mu/K$)

Q - heat rate (W)

q - heat flux (W/m^2)

R - thermal resistance (K/W)

Re - Reynolds number (GD/μ)

Sc - Schmidt number (kinematic viscosity/mass diffusivity)

Sh - Sherwood number (dimensionless mass transfer coefficient)

T - temperature (K)

V - voltage (V) or volumetric flow rate (m^3/s)

W - molecular weight (kg/kmole)

X - mass fraction (based on total mass)

Z - axial coordinate (m)

ϵ - effectiveness of wall-to-droplet heat transfer

μ - viscosity (kg/m-s)

Subscripts

2-13 - refer to locations 2 through 13 in figure 5-1

A - air property

a - atomizer

CP - constant property

E - electrical, electrode

EXP - experimentally determined quantity

G - gas phase

h - heated (test) section

I - inlet to test section

ℓ - liquid

L - loss

M - refers to either mixed-mean or mixture

O - outlet of test section

S - inside surface (wall) of test section

SAT - property at saturation state

t - transition section

V - water vapor

VP - variable property (calculated from eqn. 3-9)

W - Water

∞ - Ambient

SUMMARY

The cooling of gas turbine components has been the subject of considerable research. The problem is difficult because the available coolant, compressor bleed air, is itself quite hot and has relatively poor thermophysical properties for a coolant. Injecting liquid water to evaporatively cool the air prior to its contact with the hot components has been proposed and studied, particularly as a method of cooling for contingency power applications. The subject of the present report is the injection of cold liquid water into a relatively hot coolant air stream such that evaporation of the liquid is still in process when the coolant contacts the hot component.

Heat transfer in one-component two-phase flow has received considerable attention primarily because of steam boiler applications. Binary two-phase systems have received somewhat less attention. Both one-component and binary two-phase pipe flows have been studied with phases nominally in equilibrium at the inlet and heat input at the pipe wall. Both have been studied with phase disequilibrium at the inlet and an adiabatic boundary condition. Apparently neither has been studied with both a heated wall and significant phase disequilibrium (cold liquid and hot gas) at the inlet, the case investigated here. No method was found whereby one could confidently predict heat transfer characteristics for such a case based solely on prior studies. It was not clear whether (or to what extent)

disequilibrium between phases at the inlet would improve cooling relative to that obtained where equilibrium (i.e., complete evaporation of liquid) was established prior to contact with the hot surface.

Tests were conducted with preheated air entering a small diameter electically heated stainless steel tube. The test facility incorporated an atomizer arranged to inject a water mist into the air stream near the tube inlet. The effects of inlet disequilibrium were observed to extend downstream, first through what was interpreted as an annular-film flow regime, then through a mist flow regime, followed by a transition to single-phase in those cases for which the length of the test-section was adequate for the conditions of the test. The test results in every case showed that lower wall temperatures occurred with inlet disequilibruim. In no case was heat transfer degraded by inlet disequilibrium, either overall or locally.

1. INTRODUCTION

Consider two scenarios involving helicopters which use gas turbine engines. First, a large military twin engine/twin rotor craft loses one engine in combat, over hostile territory. This means an immediate forced landing. Second, a craft in civilian service must take off with a full load at high altitude on a hot day. Power required may exceed the safe operating limits of the engine. These scenarios would be less dangerous if a reliable contingency power capability were available.

Extra power can be obtained from a gas turbine by injecting more fuel into the combustor. This raises the turbine inlet temperature; since the device is a heat engine, thermal efficiency and power increase. However, first stage turbine blades[1] will overheat quickly. Depending on the magnitude and duration of the temperature extreme, the result may range from reduced stress-rupture life to immediate and catastrophic failure. To achieve reliable contingency power one must avoid blade overheating.

Until ceramics are sufficiently developed for turbine blade service, designers will use high-temperature metal alloys. High performance blades typically have internal cooling passages and external film-cooling holes. Air is bled from the compressor and directed to the blades to maintain reasonable surface temperatures while allowing higher turbine inlet temperature and power.

[1] In this report, "blades" refers to both the rotating and stationary airfoils in the axial flow turbine.

If water were sprayed into the cooling air and allowed to evaporate, its temperature could be greatly reduced before the mixture reached the blades. A study has shown this could allow 154% of design power (i.e. 54% contingency power reserve) with no loss of blade life.[2] Thus, a military pilot could choose a safe landing site and a civilian pilot reach cruise altitude safely.

A variation on this approach would involve injecting the water (along with the cooling air) directly into the blade. Thermal shock failure may result if liquid contacts the blade internal surfaces, but possibly the Leidenfrost effect (formation of a vapor layer between a hot surface and a liquid drop) would prevent direct contact. A more basic question is whether blade surface temperatures might be reduced further by this technique than by evaporatively cooling the air, or to the same level using less water. Two-phase cooling of internal blade passages would almost certainly be more difficult to design and use, so unless it has some significant advantage evaporative cooling should be used.

The purpose of this work is to experimentally compare heat transfer in the two cases discussed. The question to be examined is:

> For given temperatures and mass flow rates of air and water, will allowing the mixture to reach equilibrium prior to contact with the surfaces to be cooled increase or decrease cooling effectiveness?

[2] See the discussion in section 3.1 for details.

Since this was an exploratory effort, a simple geometry and boundary condition were chosen: flow in a small diameter circular tube with uniform wall heat flux. This simulates conditions in a blade with through holes. Because of the complex nature of binary two-phase flow, scaling up of the tube size was avoided even though this would have simplified certain aspects of the experimental measurements.

There is extensive prior work on single-phase flow in tubes with uniform heat flux. Some two-phase work has been done on both single-component and binary systems. However, no reports were found on heat transfer to binary two-phase flow with inlet disequilibrium; i.e., where the temperature of the gas phase was significantly higher than the liquid phase at the inlet to the heated section. The prior work on heat transfer to single component two-phase flow is for phases initially in equilibrium. The prior work on binary two-phase flow with initial disequilibrium covered flow with an essentially adiabatic wall (with heat transfer primarily between phases).

This report describes the design, construction, and testing of the experimental apparatus, data reduction methods, and the test results obtained. Subject to the limitations of the apparatus, an attempt was made to approach as closely as possible conditions which might be encountered in a turbine blade cooling application. Results were obtained for pressures to 7 atmospheres, wall temperatures to 825K, initial air temperatures to about 600K, and mass fractions to 15% water. However, the data

are not comprehensive and extrapolation to different conditions must be considered speculation.

2. STATEMENT OF PROBLEM

2.1 Idealized Problem Statement

Consider the idealized physical model shown below in figure 2-1. The large cylinder on the left is a perfectly insulated mixing chamber. It is joined to the small tube, whose wall is uniformly heated. Dry, hot air at T_A and cold liquid water at T_W are flowing into the mixing chamber where the velocity is low and pressure constant at P_M. The chamber is long enough to allow equilibrium to be reached before the mixture enters the horizontal heated tube. It is assumed that steady-state conditions prevail.

To define case 1, let M_A, T_A, M_W, and T_W be values such that at the inlet[3] the mixture is all gas phase (steam + air). The mixture at the inlet is warm, humid air (possibly saturated) at uniform temperature.

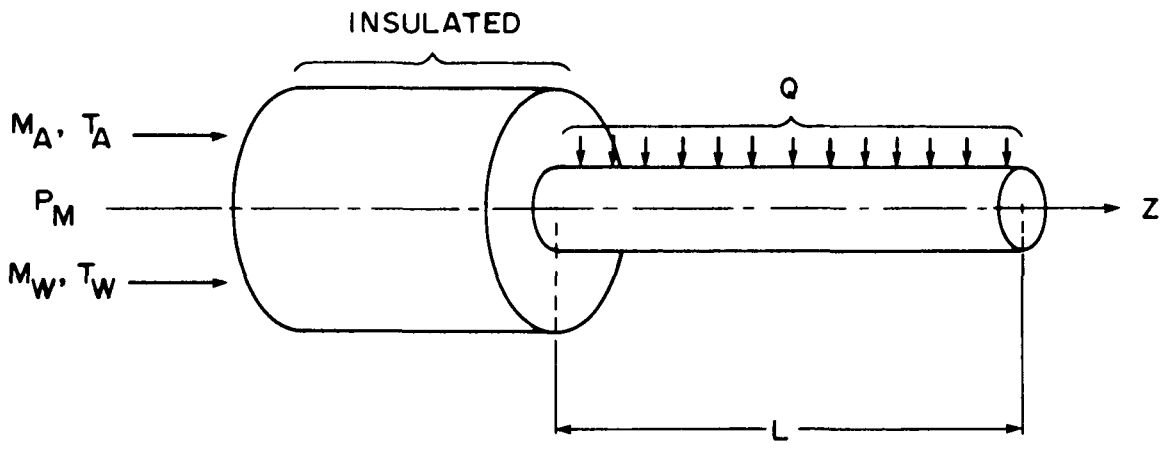

Figure 2-1 Physical Model with Inlet Equilibrium

[3]Hereafter the terms "inlet" and "outlet" will refer to the start and end of the heated section.

For case 2, consider figure 2-2. The flow rates, temperatures, and pressures of air and water at the entrance to the mixing chamber are identical with case 1. Due to the shorter mixing chamber length, there is less time for the mixture to equilibrate before reaching the inlet. The mixture at the inlet is thus warm liquid and hot, humid air (not saturated). The temperature is not uniform.

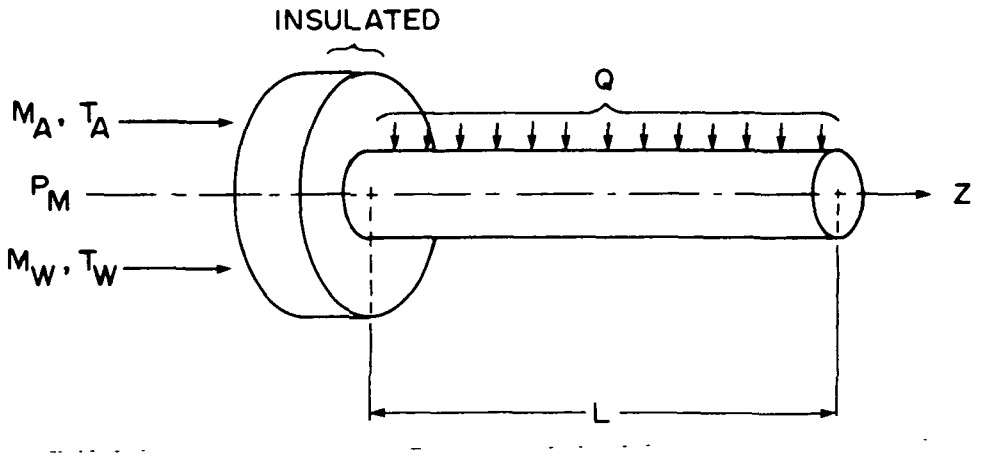

Figure 2-2 Physical Model with Inlet Disequilibrium

Cases 1 and 2 by definition have "identical entrance conditions" of T_A, T_W, M_A, M_W and P_M. Thus the total enthalpy and mixed-mean fluid temperatures for the two cases are identical at the entrance to the mixing chamber. Since the mixing chamber is adiabatic and pressure is constant, the total enthalpies and mixed-mean temperatures are constant up to the inlet to the heated section. However, the entropy is greater in case 1 since it is in equilibrium.

Within the heated section the same heat rate Q is applied uniformly over the same length L, so the total (or mixed-mean specific) enthalpies for the two cases must be identical at any point. Neglecting any difference in total pressure, the mixed-mean temperatures are also identical. This will be termed "matching local conditions" of T_M, P_M, M_A, M_W, and q_{SM}. Note that in case 1 the mass fraction of liquid (X_ℓ) at the inlet (and downstream) is zero, but is finite at the inlet in case 2. However, if the heated length and/or heat rate (L and Q) are sufficient, the outlet mixture in case 2 will be all gas phase with the same temperature profile as case 1. The outlet mixtures must therefore have the same total enthalpy, total entropy, and composition. The question to be addressed is which case will result in the lowest heated section wall temperature.

Next, consider what happens if M_W is increased without changing M_A, T_A, T_W or P_M. If the increase is large enough, some liquid will be present at equilibrium. For case 3, let M_W increase until the mass fraction of liquid at equilibrium ($X_{\ell M}$) is some small value (say 2%). All other conditions are identical to case 1. The inlet mixture is thus warm, saturated air and warm liquid water at uniform temperature.

Case 4 is identical to case 3 except that the shorter mixing chamber is used. As in case 2, equilibrium is not achieved before the mixture enters the heated section. The mixture at the inlet is hot, humid air (not saturated), and warm liquid water. The temperature is not uniform.

The same comparisons can be made as in cases 1 and 2. "Identical entrance conditions" exist by definition, and "matching local conditions" will again be present within the heated section. The outlet mixture will be gas-phase with identical temperature profiles for both cases 3 and 4 (assuming sufficient length L and heat rate Q). The four cases have identical boundary conditions (q_{SM}), but different inlet conditions (X_ℓ, T_G, T_ℓ): case 1 is single-phase at equilibrium, case 3 is two-phase at equilibrium, cases 2 and 4 are two-phase in disequilibrium. In terms of the physical model, the problem can now be stated as follows:

> For corresponding cases of "identical entrance conditions" (T_A, T_W, M_A, M_W, and P_M at the mixing chamber entrance) and specified uniform heat flux (q_{SM}), how does the wall temperature of the heated section vary with changes in inlet degree of equilibrium? Specifically as formulated here, compare the wall temperature levels and distributions for cases 1 & 2 and for cases 3 & 4.

2.2 Experimental Problem Statement

The most direct approach would be to run tests under the desired conditions and measure wall temperatures. That would require "matching local conditions" (as defined in the preceding section) for two tests, while maintaining inlet disequilibrium in one test and equilibrium in the other. Achieving such conditions poses many practical problems. For example, the idealization of

constant pressure adiabatic flow cannot be achieved in reality. Thus it would be necessary to match pressure drop and heat loss characteristics for mixing chambers of different lengths. These length differences would not be small. Evaporation times of droplets were estimated using the method of Fiszdon (1979), which indicated a mixing chamber several meters long would be needed for complete evaporation. A considerably shorter chamber would be needed for the case of inlet disequilibrium.

To avoid such problems, one might run a test with inlet disequilibrium (case 2) and measure the flow variables. Then, using a single-phase heat transfer correlation, one could calculate the expected mixed-mean and wall temperatures for the corresponding equilibrium case (case 1). Within the accuracy of the correlation, the result would be a valid comparison of wall temperatures for "identical entrance conditions" (T_A, T_W, M_A, M_W, P_M, q_{SM}), or equivalently, "matching local conditions" (T_M, M_A, M_W, P_M, q_{SM}).

The method used here differs slightly from the above description. Rather than use an existing single-phase correlation directly, single-phase dry air tests were conducted using the experimental apparatus. The data were compared to an existing correlation, which confirmed the accuracy of the measurements and data reduction techniques. This builds confidence in the results. The single-phase results were then adjusted to the "local matching conditions" present in subsequent two-phase tests by using the correlation as an interpolation

formula. The effect of any bias in the apparatus or technique is thus minimized in the comparison.

Obtaining a direct comparison of cases 3 and 4 was not possible since equilibrium at the heated section inlet, needed for case 3, could not be acheived with the facility utilized, nor would a single-phase correlation apply because some liquid would still be present at equilibrium. Cases where water mass fraction is large enough such that the equilibrium mixture contains some liquid were considered to be of secondary interest. However, for completeness, results of the measurements which were obtained for case 4 tests were, like the case 2 results, compared with corresponding case 1 results. The basis for the corresponding case 1 specification was measured data from the two-phase case 4 test, reduced to local values of total mass flow rate, mixed-mean temperature, pressure, and wall heat flux (M_M, T_M, P_M, q_{SM}). Thus, for the comparison case 1 the presence of the liquid was ignored except for its contribution to the total mass flux.

In summary, the experimental problem can be stated as follows:

> Compare wall temperatures obtained in flow situations with "matching local conditions" of total mass flow rate, pressure, mixed-mean temperature, and wall heat flux. Inlet conditions to be in one case a mixture of air and liquid water not in equilibrium, in the other air only at uniform temperature.

3. LITERATURE SURVEY

A great deal of prior work was reviewed in preparation for the tests reported here. Some prior work has been done directly related to this application, and a good deal more in closely related areas. Considerable prior work on atomization, air and water thermophysical properties, and experimental methods was reviewed as part of the experimental design process. Chapters 4 and 5 include some of the details. This discussion is limited to relevant work on water augmented gas turbine cooling, two-phase heat transfer, and single-phase heat transfer.

3.1 Water Augmented Gas Turbine Cooling

As noted in the introduction, if liquid water directly contacts the metal blade surface high thermal gradients and stresses are likely, possibly leading to catastrophic failure. Freche and Hickel (1955) studied this problem on a test engine. Five alloys of solid first stage turbine blades were modified for water injection at the blade root, with the water contacting the outside surface. Cracks or catastrophic failure occurred within 20 on-off cycles on four alloys; no failures occurred with S-816. This showed the importance of the thermal shock effect, but also that two-phase cooling may be feasible with at least one blade material. The authors noted that different heat-treatment schedules might improve thermal shock resistance of other alloys.

Van Fossen (1983) investigated the potential of evaporatively cooling compressor-bleed air for contingency power.

He used a standard computer code to model operation of a 4.5 MW (6000 shp) engine. The model featured air cooling for the compressor-drive-turbine blades in normal operation, and uncooled (solid) power-turbine blades. Various amounts of water injection into the cooling air were simulated, and complete, adiabatic evaporation assumed to calculate coolant temperature. Assuming all water evaporated prior to contact with hot components avoided the thermal shock problem. Temperature and stress-rupture life for both blade types were calculated.

At the water flow rate required to saturate the cooling air, 154% of design power was possible. A $2^1/_2$ minute transient would cause no reduction in stress-rupture life for the compressor-drive-turbine blades, but would consume about 25% of the power-turbine blade life. Of course, cooled power-turbine blades could eliminate this problem. Thermal barrier coatings were investigated and shown to be ineffective for reducing the transient temperature extreme. The projected operating conditions for the $2^1/_2$ minute transient would require approximately 32 kg (71 lb) of water. Fuel consumption was not reported.

3.2 Two-phase Heat Transfer

In two-phase pipe flow, the flow regime is the most significant variable influencing heat, mass, and momentum transfer. The regime is typically governed by the void fraction or quality, flow geometry (vertical-upwards, vertical-downwards, horizontal), and phase density and viscosity. With the

relatively small fractions of liquid studied here, annular and mist regimes result.

In annular flow the liquid flows as a film along the wall, while the gas phase flows in the center. Droplets may be entrained in the gas. In mist flow virtually all of the liquid is present as dispersed droplets. The wall may be partially wetted by impinging droplets, but is mostly dry.

Consider first the annular regime. If the flow regime in case 2 (defined in section 2.1) is annular, the heated wall is in contact with cold liquid water. In case 1 the wall is in contact with with warm, humid air. One would naturally expect lower wall temperatures in case 2. However, Freche and Hickel (1955) showed direct liquid contact can cause failure of turbine blades. Annular flow is therefore considered undesirable.

Mist flow is somewhat more complex. In a discussion of post-dryout heat transfer in one-component (steam-water) systems with uniform heat flux, Collier (1981, pp. 231-236) defines two limiting cases:

- no heat transfer between droplets and vapor
- perfect equilibrium between droplets and vapor

In the first case, the vapor mixed-mean temperature rises linearly with axial distance (the same as one would expect in single-phase flow). Wall temperature (in the fully-developed region) behaves in the same way. In the second case, the vapor temperature cannot increase until all droplets have evaporated. As evaporation proceeds, the increasing volume accelerates the

flow. This improves heat transfer from the wall, so wall temperature declines slightly with axial distance. When all droplets have evaporated, both vapor and wall temperatures rise linearly.

The second limiting case does not apply exactly to a binary (two-component) system, and both cases neglect the effect of droplets impacting the tube wall. One important conclusion can be drawn however.

In comparing cases 1 and 2 (section 2.1), note that the case 2 gas temperature is higher and velocity lower at the inlet of the heated section. Both factors will cause higher wall temperature, unless offset by the droplets. The droplets can lower wall temperature indirectly by reducing the gas-phase temperature, or directly by impacting the wall (whether or not wetting occurs).

Interaction between water droplets and heated flowing gas has been studied by Ranz and Marshall (1952), Miura, et al. (1977), and Harpole (1981). These results suggest the Ranz and Marshall correlation (or something similar)

$$Nu = 2.0 + 0.6\ Re^{1/2}\ Pr^{1/3} \qquad 3\text{-}1$$

would apply to the present study. This could be used along with conservation equations and a single-phase heat transfer correlation in a mathematical model. Rane and Yao (1981) formulated and solved such a model for turbulent mist flow in circular tubes. Their analysis was for a one-component system,

with both phases at saturation temperature at the inlet (somewhat similar to case 3). Good agreement with experimental data of others implied the model assumptions were reasonable. These assumptions included one-dimensional droplet concentration, equal diameter droplets (monodisperse), and negligible droplet/wall interaction.

Mastanaiah and Ganic (1981) included droplet/wall interaction in their model for binary two-phase pipe flow. They treated the interaction in terms of an effectiveness (ϵ) of heat exchange between wall and droplet defined as the ratio of the actual heat transferred from wall to droplet to the heat which would be required to totally evaporate the droplet. Effectiveness was assigned a value of 1.0 for $T_s < T_{sat}$ (at total pressure) and decreased according to:

$$\epsilon = \exp[1-(T_S/T_{SAT})^n] \qquad 3\text{-}2$$

They experimented with air/water mist in equilibrium (at room temperature) at the inlet (similar to case 3). When the value of n was set to 1.0 the experimental data and model showed fairly good agreement except near the inlet.

Pedersen (1970) measured ϵ for individual droplets impinging normally on a pre-heated plate in the absence of airflow. He observed two distinct regions: wetting with ϵ of about 90%, and non-wetting with ϵ of about 15%. A fairly sharp transition occurred at about 530K (500F). The transition temperature was influenced by impact velocity, as was effectiveness in the non-

wetting region. This suggests a more detailed model than 3-2 might give better agreement with experimental results.

A study similar in many respects to the current work was performed by Mori, et al. (1982), who experimented with air-water mixtures flowing in a small-diameter electrically heated tube. Although turbine-blade cooling motivated their research, the air and water were introduced at the same temperature (ambient) again similar to case 3. In an aero-engine the air would be considerably hotter than the water.

A stainless-steel tube of 1.8 mm I.D. and 2.0 mm O.D. was mounted vertically between electrodes, with a mixing tank at the upper end. Compressed air was measured and fed to this tank, where water was injected through a needle concentric with the tube axis. Thermocouples welded directly to the tube wall measured temperature. No mention is made of how fluid temperatures were determined. Tests were conducted with straight tubes 150 and 300 mm long, and a tube 920 mm long coiled into a helix. The coiled tube was used in an attempt to simulate the Coriolis effect in a rotating gas turbine blade.

With straight tubes, wall temperatures were low and almost constant near the inlet, followed by a region of steeply rising temperature, and finally a region of linearly rising temperature. These results were interpreted as indicating regions of annular flow, mist flow, and single-phase flow. In the mist region, a slight wall temperature fluctuation was observed. Some runs were interpreted as having a direct transition from annular to single-

phase flow, without any mist region. The data in the single-phase region were shown to agree with a single-phase heat transfer correlation. The results for the coiled tube tests were similar, but with substantial temperature variations around the tube circumference.

Film thickness in the annular region was estimated using a force balance. From this the film flowrate, film surface temperature, and interfacial heat flux were calculated. By assuming all interface heat flux was used for evaporation, a Sherwood number was calculated. This was shown to be a function of the cumulative heat supplied per unit mass, and was asymptotic to the correlation

$$Sh = 0.022\ Re^{0.8}\ Sc^{0.4}. \qquad 3\text{-}3$$

This apparently confirms the analogy between single-phase heat and mass transfer.

The calculated liquid film flow rate was plotted against gas velocity, and compared to a correlation for critical film flowrate (Kutateladze and Sorokin, 1969). Below the critical flowrate, the film is stable and simply evaporates. Thus the flow changes directly from annular to single-phase. Above the critical value, interfacial shear forces cause instability in the film. Considerable liquid is entrained as droplets, leaving mist when the remaining film evaporates. The results of Mori, et al. were consistent with the trend of the correlation, but not with the magnitude of the critical film flowrate. The authors

speculated that high surface-tension forces (due to the small tube diameter) increased film stability.

Major differences between the work of Mori, et al. and the present work are: (1) they introduced air/water mixtures in a near equilibrium state primarily under conditions such that the equilibrium state was saturated with liquid water present, whereas the present work is for highly nonequilibrium two-phase air/water mixtures at the inlet and includes mixtures whose corresponding equilibrium state is an all gas mixture (similar to case 2, section 2.1); and (2) the present tests were performed such that tube wall temperatures measured using the two-phase mixtures to cool the surface could be compared directly to wall temperatures which would occur were the same mixture to reach equilibrium before cooling the surface.

In addition to pipe flows, investigators have analyzed and/or experimented with binary mist flow over flat plates (Heyt and Larsen, 1971; Hishida et al., 1980 & 1982), over cylinders (Kuwahara et al., 1982), and in jet impingement geometries (Goodyer and Waterston, 1974; Viannay et al., 1978). All of these have introduced the air and water at virtually ambient conditions (T_A, $T_W \approx 295$ K, $P_M \approx 100$ kPa) and except for Goodyer and Waterston used relatively cool surfaces ($T_S \approx 375$ K). Apparently the study of binary mist flow heat transfer with initial disequilibrium ($T_G >> T_\ell$) and high surface temperature is without precedent.

3.3 Single-phase Heat Transfer

For comparison with two-phase results, data from corresponding single-phase tests were needed. As noted in section 2.2, it was impractical to exactly match test conditions. Instead, single-phase (air only) data over a range of Reynolds numbers, temperatures, and wall heat fluxes were collected. This data was adjusted to "matching local conditions" (T_M, P_M, M_M, and q_{sM}) present in the two-phase tests using the form of an existing single-phase heat transfer correlation as an interpolation formula. Additionally, directly comparing the existing correlation with the single-phase results showed good agreement. This provided confidence in both the single-phase and two-phase results, since the same apparatus and similar procedures were used for both types of test.

Single-phase turbulent pipe flow heat transfer has been widely studied. Both local and average (over a substantial tube length) heat transfer correlations are available. For the purpose of adjusting results, it was necessary to consider local heat transfer coefficients. These often take the form $Nu = f(Z/D) \times g(Re,Pr)$, where the function $g(Re,Pr)$ represents the Nusselt number for the hydrodynamically and thermally fully-developed case. Many correlations for the fully-developed Nusselt number exist with none clearly superior.

A number of investigators have reviewed the work of others, attempting to find equations which accurately correlate most of the reliable data. An excellent example is the study by Sleicher

and Rouse (1975). Their review covered both the constant fluid property (small radial fluid temperature variation) and variable property cases, for fully developed flow. Several schemes for accommodating variable properties were considered; the recommendation for use with gases was a correction factor to the constant property Nusselt number:

$$(Nu_{VP}/Nu_{CP}) = (T_S/T_M)^n \qquad 3\text{-}4$$

$$n = -\log_{10}(T_S/T_M)^{1/4} + .3 \qquad 1 < T_S/T_M < 5$$

$$10^4 < Re < 10^6 \qquad 0.6 < Pr < 0.9 \qquad 40 < Z/D$$

This is as reported by Sleicher and Rouse. The equation for n is somewhat ambiguous, with two possible interpretations:

$$n = -\log_{10}\{(T_S/T_M)^{1/4}\} + .3 \qquad 3\text{-}5$$

$$n = -\{\log_{10}(T_S/T_M)\}^{1/4} + .3 \qquad 3\text{-}6$$

Trial calculations show that n determined from 3-5 is positive, and the correction declines with increasing temperature ratio. One would expect a correction needed because of temperature variation would increase as the temperature ratio increased. Equation 3-6 gives negative values for n, and the correction increases with increasing T_S/T_M.

Kays and Crawford (1980, p. 281) reviewed the Sleicher and Rouse result. They did not note the ambiguity, but presented the result in the form of 3-6, and recommended simplified approximations for turbulent pipe flow of a gas;

$T_S/T_M > 1$ $\quad n = -0.5$ (heating)

$T_S/T_M < 1$ $\quad n = 0.0$ (cooling)

This further confirms that 3-6 is the correct form.

Kays and Crawford (1980, pp. 238-243) also presented a semi-empirical analogy for fully-developed flow of a constant property gas ($Pr \approx 1.0$) in a tube with uniform heat flux. Although their equation shows excellent agreement with some experimental data, it is cumbersome and they suggest a simpler approximation;

$$Nu_{CP} = 0.022\ Pr^{0.5}\ Re^{0.8}. \qquad 3\text{-}7$$

This is similar to the Dittus/Boelter correlation (often utilized, although it is for the average, not local Nusselt number), recommended by McAdams (1954, p.219):

$$Nu = 0.023\ Pr^{0.4}\ Re^{0.8} \qquad 3\text{-}8$$

In the present study, the Kays and Crawford correlation for a constant property gas is used, modified by the Sleicher and Rouse correction factor for variable properties:

$$Nu_{VP} = 0.022\ Pr^{0.5}\ Re^{0.8}\ (T_S/T_M)^n \qquad 3\text{-}9$$

$$n = .3 - \{\log_{10}(T_S/T_M)\}^{1/4}; \quad 1 < T_S/T_M < 5$$

$$n = 0; \quad T_S/T_M \leq 1$$

$$10^4 < Re < 10^5 \quad 0.6 < Pr < 0.9 \quad 40 < Z/D.$$

All fluid properties in 3-9 are evaluated at the mixed-mean temperature.

4. EXPERIMENTAL APPARATUS AND PROCEDURE

4.1 Apparatus

The experimental apparatus consisted of the seven major systems indicated in figure 4-1 below. Air and water supply systems provided measured air and water at controlled temperature and pressure to an atomizer. The atomizer produced a mist at the inlet to a test section, which was a small stainless-steel tube heated by AC current flowing in its wall. The test section discharged into an exhaust system. A power supply system provided the air preheater and test section power. An instrumentation system measured and recorded all temperatures. Pressures, flow rates, and power input were read and recorded manually. Detailed descriptions of the test section and atomizer follow, along with a brief description of the instrumentation.

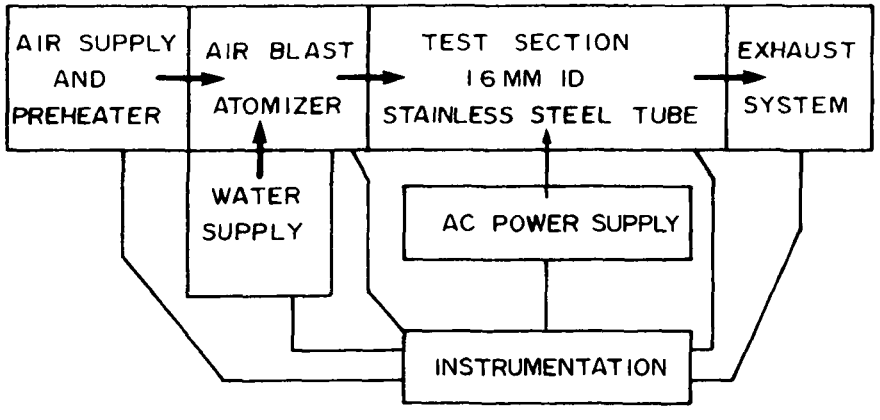

Figure 4-1 Apparatus Block Diagram

4.1.1 Test Section--The test section is shown in figure 4-2. It was constructed of type 304 stainless-steel tubing, 1.6 mm I.D. and 1.8 mm O.D. A section of this tubing was brazed to copper electrodes spaced 150 mm between centers, and cut to fit into the atomizer unit. Five commercial chromel/constantan thermocouples were mounted to the tube wall using Omega CC high temperature cement. All of these thermocouples were sheathed in stainless-steel tubing of either 0.25 or 0.50 mm O.D., with the measuring junction not grounded to the sheath material. The leads were wound helically around the tube to minimize conduction loss. The test section was insulated with layers of ceramic fiber batting, fiberglass batting, and an outer jacket of aluminum foil. Total insulation thickness was about 100 mm. A tee fitting (not shown in figure) with thermocouple was installed at the test section outlet to measure exit mixture temperature.

The electrodes were mounted on a bakelite baseplate to isolate the test section from possible short-circuits. A dielectric gasket material was used between the atomizer unit and the test section. The test section was horizontal, with the wall thermocouples mounted at the horizontal centerplane.

AC power was used to heat the tube wall for ease of control. With AC power, thermocouples can be welded directly to the surface, but the readout instrumention must be able to filter out the 60 Hz noise which is imposed on the signal.[4] Shielded,

[4]With DC heating, thermocouples cannot be welded directly to the surface without special provisions. See for example Dutton and Lee (1959).

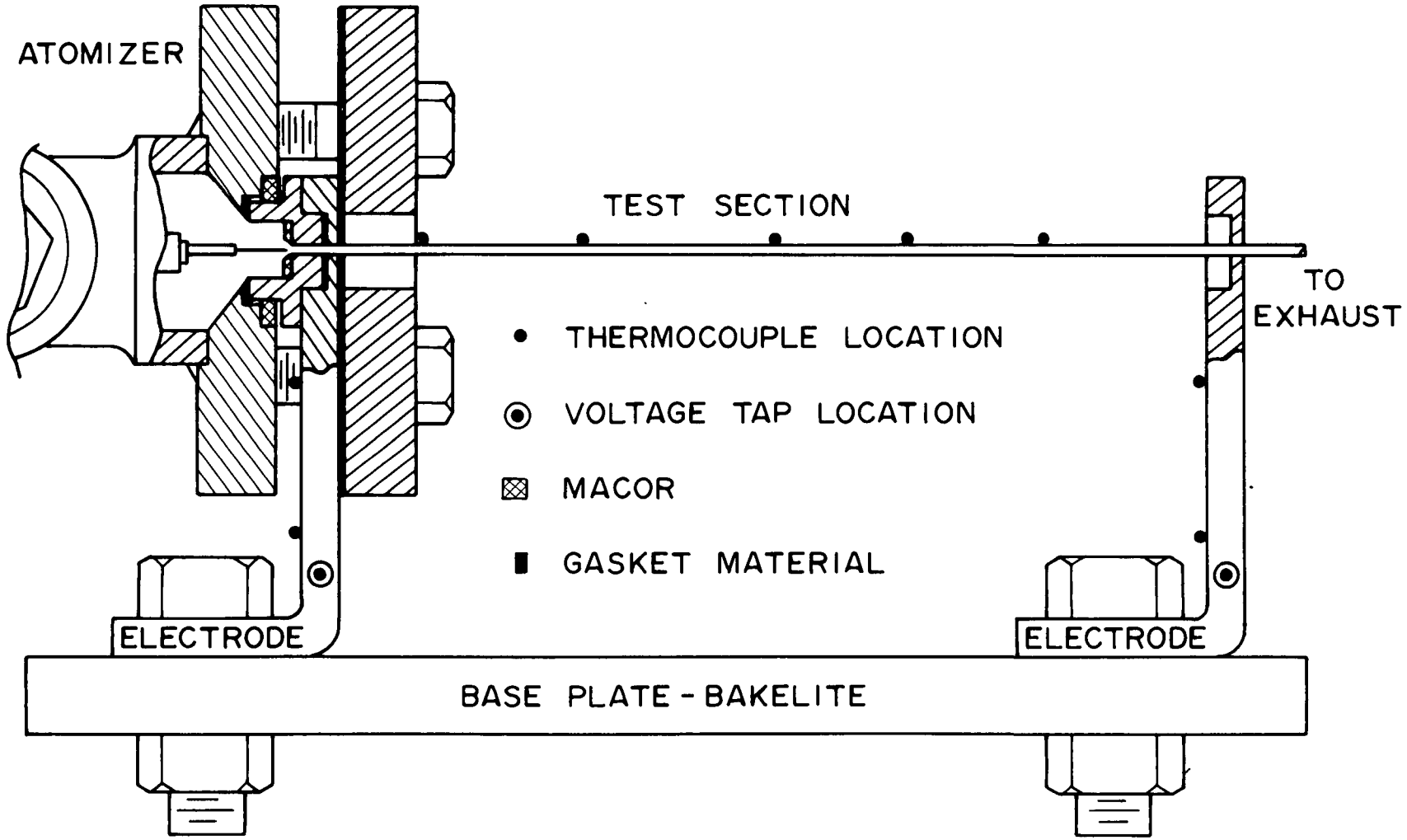

Figure 4.2 Test Section

ungrounded thermocouples were used to allow use of an electronic data logger.

To carry the heating current without significant power loss, the electrodes were large in relation to the test section tube. Although of reduced thickness at the joint with the tube, it was felt they could be significant conductors of heat between the test section and ambient. Therefore, two copper/constantan thermocouples were mounted on each electrode to aid in estimating this heat loss.

4.1.2 Atomizer--The atomizer design requirements were rather special. Typically an atomizer produces a mist with a range of droplet sizes, and varying the pressure or flow rate will cause this range to shift. For these tests, a size distribution independent of flow variables was desired. Perhaps the most severe requirement was the need to use high temperature air. This required careful design to minimize heat transfer between the water and air passages. Operation at high pressures (perhaps eventually up to 1500 kPa) was anticipated. The atomizer was to exhaust into the test section, but with the option of interposing a transition section of variable length. This would allow the non-equilibrium mixture to approach equilibrium prior to the inlet, so the effect of the degree of disequilibrium could be studied (this has not yet been done). Finally, because the test section would be conducting a heating current, a pressure-tight,

dielectric joint was needed between the atomizer and test section.

Many types of atomizers are commercially available. Dombrowski and Munday (1968) review the characteristics of several of the most common. Four possible types were considered; they are summarized here. The first is often referred to as a pressure atomizer. It consists of a small orifice through which liquid is forced at high pressure. The free jet of liquid forms a cone shape, which of course has increasing surface area as the jet moves downstream. Eventually the cone breaks up into filaments and then droplets as surface tension forces grow. This type is characterized by a rather wide droplet size distribution, rather large droplets, and narrow range of flow rate for good atomization. These features made it unsuitable.

The second type reviewed was the centrifugal atomizer. This type uses a spinning disc or cup, with liquid fed to the center and being flung from the rim. It can be designed to produce consistent droplet sizes, but in general is for higher liquid flow rates than needed here. Also the spray pattern tends to be a flat disk, which could not be directed easily into the test section.

A third type, used extensively in aerosol research, uses an ultrasonic signal to stabilize the break-up of a liquid jet. Liu and Lee (1977) describe the design and operation of a commercially available atomizer of this type. It can produce a single droplet diameter (monodisperse), with very exact control

over flow rates. However, the flow rate of liquid is very small. About 100 of these would have been required to provide sufficient flow.

The fourth type is sometimes referred to as an air-blast or two-fluid atomizer. This was the design used. It can be seen in cross-section in figure 4-3. This type produces concentric jets of water and high velocity air. Momentum transfer to the water jet provides the mechanism for break-up into droplets. Several papers on air-blast atomizer design were consulted, including the PhD thesis of G. Lorenzetto (1976). The final design was a compromise between predictability of performance, flow and mounting requirements, and simplicity of construction.

The main body consisted of a 19 mm ($^3/_4$ in.) pipe tee fitting, with an 83 mm ($3^1/_4$ in.) diameter, 12 mm ($^1/_2$ in.) thick flange welded to the downstream end. The flange was counterbored to accept a transition section, which contained the air nozzle. Air entered the atomizer from the left in figure 4-3 passing straight through to the air nozzle. A chromel/constantan thermocouple monitored the preheated air temperature near the atomizer inlet (see T2 in figure 5-1). Water entered from the bottom, via a 6 mm ($^1/_4$ in.) diameter tube. The tube was bent 90° and positioned in line with the center of the air nozzle. The end of the tube was threaded to accept a water injection needle, which was positioned with its tip (orifice) very near the throat of the air nozzle. The exact location of the needle tip was adjustable by means of shims. Water temperature was measured

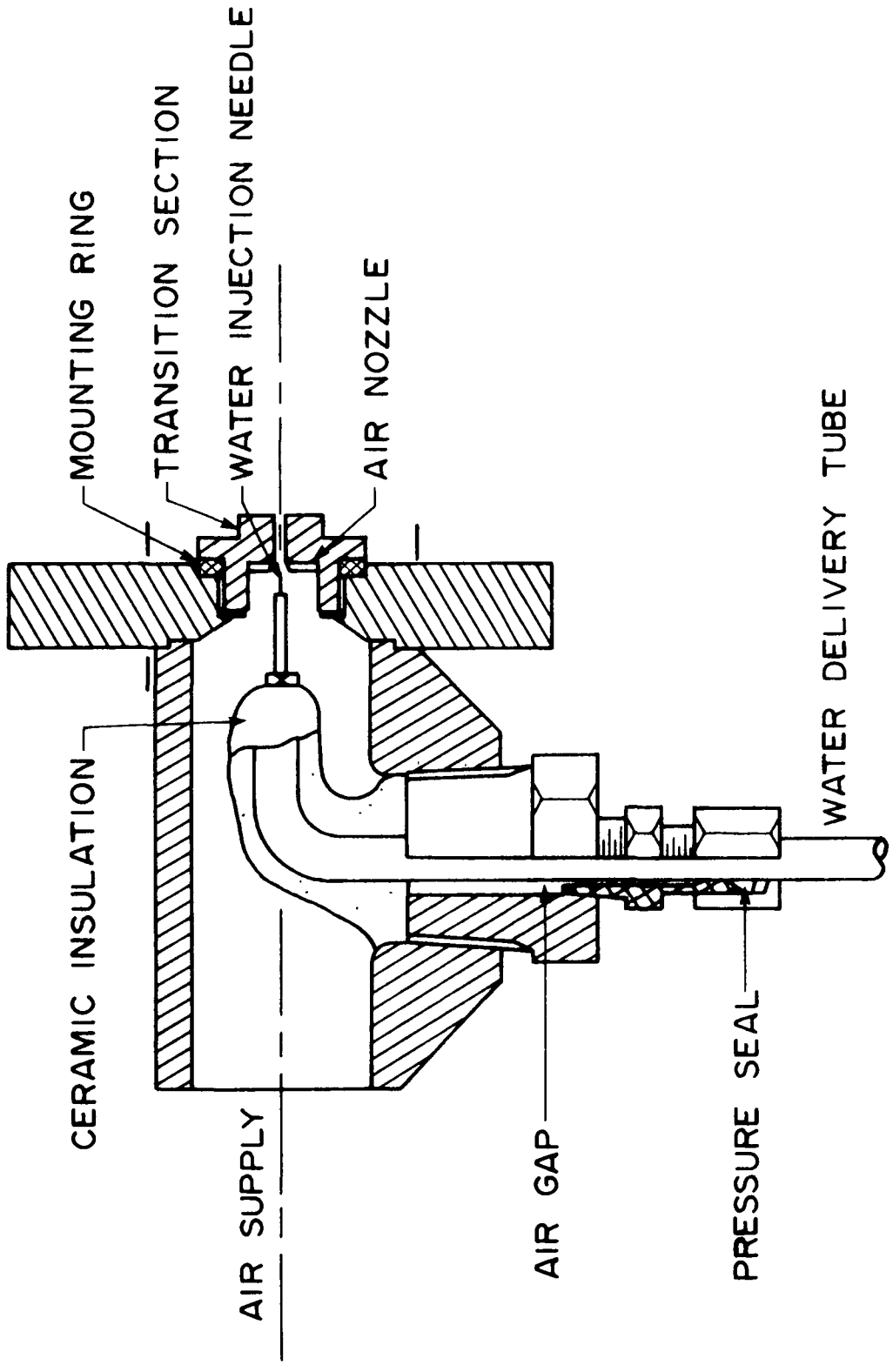

Figure 4-3 Atomizer

at the centerline of the water delivery tube immediately upstream of the water injection needle by a copper/constantan thermocouple (see T3 in figure 5-1). For the test results reported here the air nozzle throat diameter was 1.5 mm and the water injection needle orifice diameter was 0.20 mm. Estimates based on an empirical correlation of Lorenzetto (1976) showed that these air nozzle and water orifice diameters should produce a mist with a droplet Sauter mean diameter of the order of 10 μm that would remain relatively independent of air and water flow rates over the range covered by the present tests.

The water delivery tube was mounted to the atomizer by a tube fitting, passing through a pipe plug. All direct mechanical contact was avoided to minimize heat transfer to the water, but it was necessary to have a pressure seal at the tube fitting. The tube was coated with ceramic fiber insulation in putty form after installation. Even with these precautions, boiling within the tube occurred in cases with high air temperature and the lowest water flow rates.

All parts of the atomizer and transition section were of type 304 stainless steel, with two exceptions. A transition mounting ring and the air nozzle were constructed of MACOR, a machinable glass-ceramic. To minimize evaporation prior to the test section, droplet impingement on metal surfaces was to be avoided wherever possible. The air nozzle was the only surface where MACOR could be substituted. The MACOR transition mounting

ring and gasket provided the required dielectric joint between the atomizer and the test section.

The design of the atomizer provides for inter-changeable water injection needles, air nozzles, and transition sections. This allows the same basic apparatus to be used for studying a wide range of mass flows, mass ratios, test section diameters, and the additional variable of nominal adiabatic mixing length prior to heated length. All tests reported here used the minimum adiabatic length. A long transition was simulated by comparing with single-phase air only data taken at similar conditions (see section 2.2).

4.1.3 Instrumentation--All temperatures were measured by thermocouples. Those monitoring intermediate ($100 < T < 400$ C) and high temperatures ($T > 400$ C) were calibrated. A steam point was used for an absolute standard. For high temperature calibration (to 700 C) a thermocouple furnace was used. All junctions were inserted into a copper block and placed in the furnace. The intermediate temperature junctions were calibrated in the same apparatus using one of the high temperature junctions as a standard. The low temperature junctions were not individually calibrated. However, prior experience with junctions made from the same rolls of wire indicated very close agreement with standard tables below 100 C.

All thermocouples were used with reference junctions immersed in an ice bath. Readings were made by a microprocessor-

controlled data logger capable of resolving to 1 μV. Also included in the circuitry was a hand-balance potentiometer for verifying the readings. Readings were converted to temperature using cubic-spline interpolation from tables.

Water flow was measured by a calibrated rotameter. Volumetric air flow rates were measured using Vol-O Flow meters and rotameters calibrated against the Vol-O-Flow meters. The Vol-O-Flow meter design divides the airflow among multiple small parallel channels to produce a laminar flow pressure drop. The manufacturer's calibration was used for these devices. Air density was determined from pressure and temperature measurements and an equation of state (Vasserman et al. 1971). Air pressures were determined by calibrated Bourdon-tube gages.

Test section voltage drop and current were measured with a digital multimeter. Since AC current was used, the effective test section power input was found by multiplying RMS voltage by RMS current. The multimeter read true RMS voltage, so no corrections were required. The same multimeter had been used in prior experiments with water flowing in a similar apparatus. The results showed good agreement between energy balances based on thermal vs electrical measurements.

4.2 Experimental Procedure

The procedure described below was developed to minimize uncertainty in the results. Any error in procedure, leak, or loose connection could render the data useless. Except for

verifying reproducibility, the need to repeat a series of test runs was to be avoided because of the time and effort required to acheive a desired steady-state condition. Thus, many steps were taken to verify the apparatus, recalibrate some instrument, or otherwise check for problems before proceeding.

To clarify the following description, some definitions are in order. A complete set of readings from all instruments will be termed a data "set." Typically three or more data sets were recorded with no deliberate changes in controlled parameters. This verified steady conditions were present. Such a group of data sets will be called a test "run." On completion of a run, a deliberate change in a single controlled parameter (usually either the power input level or water flow rate) was made. A sequence of such test runs constituted a test "series."

A typical series included calibration runs with air only and no test-section power input, single-phase runs with air only and a heated test-section, and three two-phase runs with nominally 5, 10, and 15% water by mass. The following description will progress through a series chronologically.

4.2.1 Preliminaries--The first step was to verify thermocouple circuitry and calibration. With only ambient temperature air flowing, no power applied to the test section, the exhaust system condenser cooling water flowing, and the condensate drain valve closed, the apparatus was left to equilibrate for several hours. Then temperatures were read on

both the data logger and the hand balance potentiometer. If these were all consistent at ambient levels, the procedure continued.

The air flow rate and air preheater control were next adjusted for the desired atomizer inlet air temperature and mass flow rate. After several hours conditions stabilized, and the thermocouple check was repeated to verify circuitry and calibration. The apparatus was then ready for the first run.

4.2.2 Air Only Runs--For the first run, the data logger was set to automatically record at thirty minute intervals. When it started a scan, pressure and flow readings were recorded manually on the paper tape output. At least three data sets were recorded before applying power to the test section. This constituted a zero-power calibration run. From this data estimates of the rate of heat loss to ambient from the test section, transition section, and atomizer were made (as described in section 5.2).

Next, power was applied to the test section. This caused the air flow rate to change. After readjusting the metering valve to maintain the flow rate, several hours elapsed before steady conditions prevailed. The data logger was again set for thirty minute intervals, and other readings taken as before. This run also included at least three data sets. The test section power was then shut off, but air flow and preheater power left on (overnight).

4.2.3 Nominal 5% Water Run--This run typically commenced on the following day. Prior to applying power to the test section, a calibration run was conducted as before. In addition to verifying thermocouple circuitry and calibration, this data established the rate of heat loss (section 5.2).

Next, the water flow was started, the exhaust section condensate drain opened, and power applied to the test section. Adjustments to the air metering valve, water metering valve, and air preheater power level were required to maintain the desired conditions. Several hours after the final adjustments, readings commenced in the same manner. Typically, at least three data sets were recorded, comparing them to assure steady conditions prevailed. Following the final data set, test section power and water flow were shut down, leaving the preheated air flowing (again overnight).

4.2.4 Nominal 10% & 15% Water Runs--These runs were usually taken together on the the day following the 5% water runs. The procedure duplicated that above, except that after recording the final data set at 10% the water flow was increased to 15%. At this level, steady conditions were reached in about thirty minutes. Thus, the final run at 15% required only about two hours following completion of the 10% run.

4.2.5 Shutdown--Upon recording the final set, the water and power to the test section were shut off. After some time, the exhaust section condensate drain stopped discharging water and

was closed. Then, the air preheater power was cut, and the air flow slowly cut to zero by closing air exhaust valve. Finally, as the system pressure level reached a suitable value the air inlet valve was closed. The air supply section, test section, and exhaust section were thus sealed and pressurized. By observing the pressure drop, it was possible to estimate the rate of air leakage. The rate was always less than 1% of the total air flow.

5. DATA REDUCTION

As described in the experimental problem statement, section 2.2, the objective was to measure wall temperatures for two-phase tests with disequilibrium at the inlet. These were to be compared with wall temperatures for single-phase tests (here air-only) at "matching local conditions" of mixed-mean temperature[5], pressure, total mass flow rate, and wall heat flux (i.e. T_M, P_M, M_M, and q_{SM}). Since obtaining precisely matching conditions for specific test cases was impractical, air-only test results at similar conditions were to be interpolated to match the exact two-phase test conditions. It was also desired to determine the local heat transfer coefficients for each test as normally defined for a single phase internal flow; i.e.,

$$h(Z) = q_{SM}(Z)/\{T_S(Z) - T_M(Z)\} \qquad 5\text{-}1$$

In order to carry out the above procedures it was necessary to determine values of T_S, T_M, P_M, M_M, and q_{SM} at each tube wall thermocouple location along the test section for each test run. These thermocouples were cemented to the outer surface of the tube wall. The temperature drop across the wall ($\simeq$ 1 K) was neglected since it was not significant in comparing surface temperatures for local matching conditions; and for air-only

[5] Temperature for the non-equilibrium state was defined as the equilibrium temperature of a mixture of identical composition and total enthalpy, at the same total pressure. This is the temperature the test mixture would have attained were it allowed to equilibrate adiabatically.

tests, which were compared with a prior correlation, the drop was only $\simeq$ 1% of $T_s - T_m$. Since steady-flow conditions prevailed, M_M was constant for a given test run, and was calculated as the sum of the individually measured values of air and water flow rates.

Determination of q_{SM}, T_M, and P_M required more extensive analyses. These are outlined in the following sections. With the above noted quantities determined, local dimensionless variables Re, Pr, and Nu were evaluated. The specific method of adjusting the air-only data to the required matching conditions is given later in section 6.5. The present chapter concludes by indicating several checks which were performed to establish the validity and consistency of the data, followed by a discussion of experimental uncertainties associated with the reduced data.

5.1 Heat Fluxes

The local heat source (q_E) was approximately uniform due to the use of electric resistance heating. The average value was determined by measuring the current and voltage drop across the test section. Two corrections were applied to determine the net local heat flux (q_{SM}); the first accounted for variation of electrical resistivity with temperature (up to 20% from inlet to outlet), the second for heat lost to ambient through the insulation ($q_{S\infty}$).

To correct for variable electrical resistivity, total tube wall resistance was computed from the voltage drop and current measurements for all air-only runs. This resistance was

correlated against average tube wall temperature, giving a linear relation ($V/I = aT_S + b$). The data points fell within 1.5% of the correlation and were consistent with published values for type 304 stainless steel. Local heat source was calculated from measured current and local resistivity determined using the linear relation. A small uniform adjustment was then applied so the integrated local heat source would be consistent with the directly measured overall value which was considered to be known with higher confidence than the local values:

$$q_E(Z) = I^2\{aT_S(Z)+b\}/\pi DL + q_{corr} \qquad 5\text{-}2$$

where $$q_{corr} = \left\{ VI - (I^2/L)\int_0^L \{aT_S(Z)+b\}\, dZ \right\}/\pi DL$$

The correction for test-section loss to ambient ($q_{S\infty}$) was calculated assuming one-dimensional conduction through a thermal resistance (R_h). The determination of the thermal resistance is described in Appendix B. The correction varied from 3% to 6.5% of the total electrical input for single-phase tests and from less than 1% up to 3% for two-phase tests, and was applied at each axial thermocouple station:

$$q_{S\infty}(Z) = \{T_S(Z)-T_\infty\}/\{R_h \pi DL\} \qquad 5\text{-}3$$

$$q_{SM}(Z) = q_E(Z) - q_{S\infty}(Z)$$

5.2 Local Flow Variables

Local mixed-mean fluid temperatures were determined by energy balances between the start of the heated length (labled

INLET in figure 5-1) and each wall thermocouple station. Given an inlet enthalpy, the determination of which is outlined in a later paragraph, local heat flux [$q_{SM}(Z)$] was numerically integrated to find the mixture enthalpy at the thermocouple station. From this, the mixed-mean temperature was determined by using the following system of equations (for two-phase tests):

$$\begin{aligned} P_V &= P_{SAT}(T_M) \\ X_{VM}/X_A &= \{P_V/(P_M-P_V)\} \times \{W_V/W_A\} \\ X_W &= X_{VM} + X_{\ell M} \\ i_M &= X_A i_A(T_M, P_M-P_V) + X_{VM} i_V(T_M, P_V) + X_{\ell M} i_\ell(T_M, P_m) \end{aligned} \qquad 5\text{-}4$$

The four unknowns were P_V, X_{VM}, $X_{\ell M}$, and T_M. Mass fractions of water and air (X_W & X_A) were known from measurements of flow rates, and the mixture pressure (P_M) was assumed to vary linearly between inlet and outlet measurements. Enthalpies were calculated using equations of state for water and air (Meyer, et al. 1977 for water; Vasserman et al. 1971 for air). Assuming a mixture temperature (T_M) allowed progressive solution to find enthalpy (i_M). A zero-finding algorithm was used to determine the temperature from the known enthalpy.

System 5-4 applied with liquid present. With water present only as vapor, the system simplifies to

$$\begin{aligned} X_W/X_A &= \{P_V/(P_M-P_V)\} \times \{W_V/W_A\} \\ i_M &= X_A i_A(T_M, P_M-P_V) + X_W i_V(T_M, P_V). \end{aligned} \qquad 5\text{-}5$$

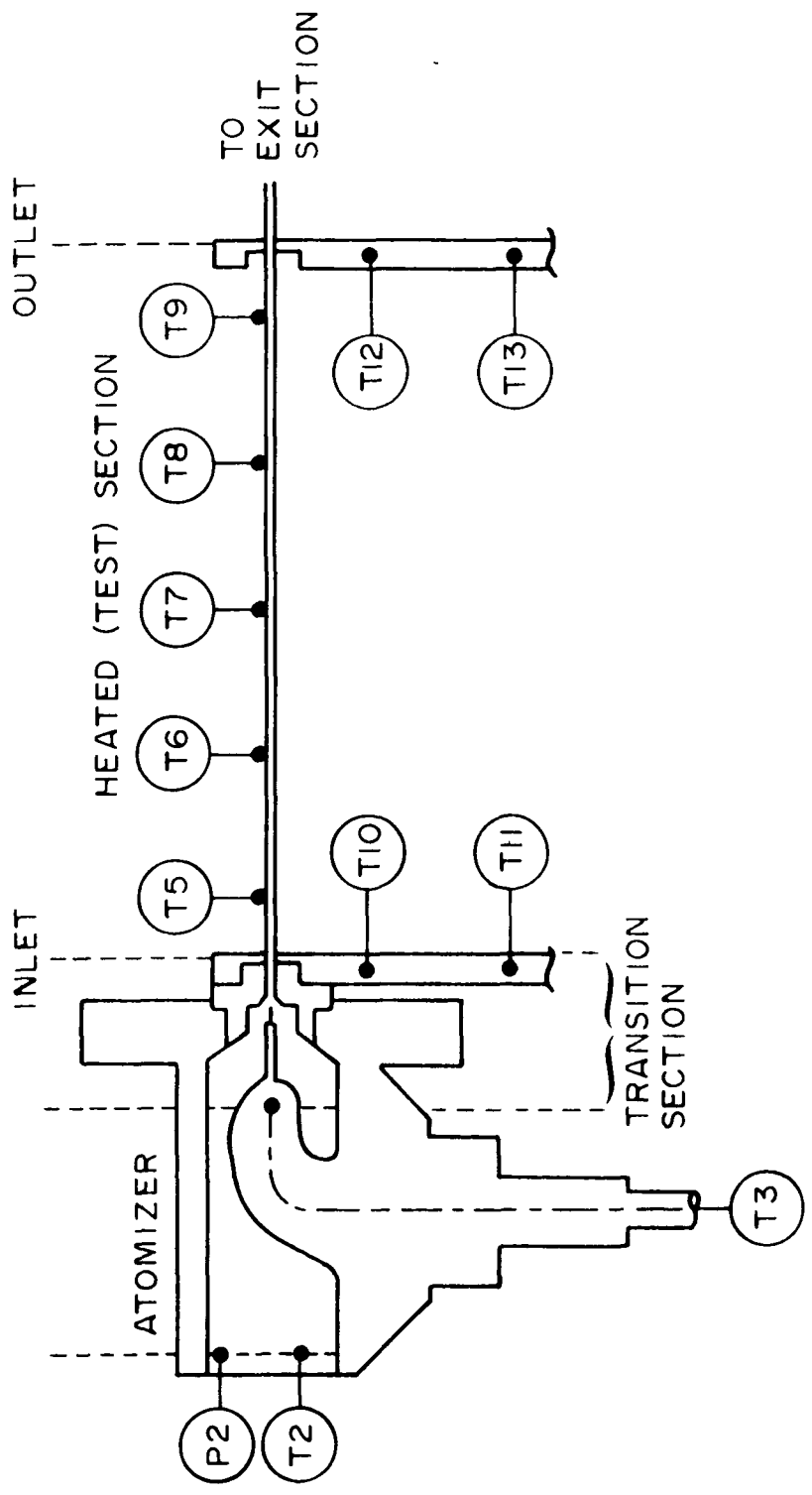

Figure 5-1 Overall Schematic

Here the only unknowns are T_M and P_v. The first equation can be solved once for P_v, then the second iteratively for T_M. In practice, the first equations of each system were solved for P_v. If 5-4 resulted in the smaller value of P_v the presence of liquid was indicated. If 5-5 resulted in the smaller value, superheated water vapor was indicated. If the values were identical, saturated vapor was indicated. The formulation needed to determine temperature in air-only tests is an obvious special case of 5-5.

The solution of the applicable system gave the mixed-mean temperature T_M. This was the total or stagnation temperature. In high velocity flow, the adiabatic wall temperature is used rather than stagnation temperature for defining heat transfer coefficients. A one-dimensional flow model (Shapiro, 1953, pp.75-85) was used to estimate the compressibility effect on single-phase data. The estimates ranged from 0.1 to 1.0 K, so the effect was neglected.

Knowledge of T_M, T_S, and q_{SM} permitted the determination of h(Z) from equation 5-1. Further, X_w, $X_{\ell M}$, T_M, and P_M fix the thermodynamic state of an equilibrium mixture. Thus, the local fluid properties (viscosity, specific heat, and thermal conductivity) could be determined. This was done using property equations for dry air at T_M and P_M (Vasserman et al. 1971).

This approach assumes the thermophysical properties of dry and humid air are identical. Richards and Florschuetz (1983) have shown this is a reasonable approximation at low values of

humidity. For the largest mass fraction of water vapor occurring in any single phase flow regime in the present study (about 10%), the neglect of humidity reduces the value of h by only 5%.

At this point, all quantities were available to determine local dimensionless variables Re, Pr, and Nu:

$$Re = GD/\mu_A(T_M, P_M) \qquad 5\text{-}6$$

$$Pr = \mu_A(T_M, P_M) \times C_{P_A}(T_M, P_M) \; / \; K_A(T_M, P_M). \qquad 5\text{-}7$$

$$Nu_{EXP} = hD/K_A(T_M, P_M) \qquad 5\text{-}8$$

Here G is the total mass flux and h is defined by equation 5-1.

Returning to the determination of the enthalpy at the start of the heated section, reference is again made to figure 5-1. Fluid temperature measurements at that location (labled INLET) were not practical because of the small tube diameter and two-phase mixture. Indeed, it was found that readings of a thermocouple installed slightly upstream of the water injection orifice in the air flow at station 3 were significantly affected when water injection was initiated. Instead, the preheated air temperature was measured at station T2 where it was found to be unaffected when water injection was initiated. Water temperature was measured at station T3. For two-phase tests the enthalpy at the INLET station was then calculated from the following energy balance:

$$i_{MI}(M_A + M_W) = M_W i_\ell(T_3, P_3) + M_A i_A(T_2, P_2) - Q_{La} - Q_{Lt}. \qquad 5\text{-}9$$

In this equation Q_{La} and Q_{Lt} are the heat losses from the two system subsections specified in figure 5-1 as ATOMIZER and TRANSITION SECTION. Their evaluation is detailed in Appendix B. Q_{Lt} ranged from 1 to 6% of the electrical power input. Q_{La} ranged from 5 to 10% for most runs, but reached about 30% in several cases.

For single phase air-only tests it was possible to use thermocouple T3 for a valid measure of air temperature, so that for these tests the INLET enthalpy was computed from:

$$M_A i_{MI} = M_A i_A(T_3, P_3) - Q_{Lt}$$

where Q_{Lt} ranged from 3 to 10% of the electrical power input.

5.3 Data Checks

For single-phase tests the thermocouple located in the water delivery tube (T3 in figure 5-1) could be used to measure the air temperature at the entrance to the transition section. In addition, a thermocouple was mounted just downstream of the heated tube in the exit section (not shown in figure 5-1). This thermocouple measurement was not used in the primary data reduction procedure described in the preceding sections. An overall energy balance carried out for each single phase test based on these two temperatures, the air flow rate, the measured electrical power input, and the calibrated thermal losses closed to better than 4% in every case.

Two additional comparisons also provided confidence in the reduced data. (1) For single-phase air-only tests Nusselt numbers were found to be consistent with an existing empirical correlation for fully developed turbulent pipe flow. (2) For two-phase air/water tests with inlet disequilibrium no prior results were available for comparison. However, as liquid water evaporated in the mixture flowing along the tube, a single-phase flow condition was approached. For the present tests at low water mass fraction, Nusselt numbers and tube surface temperatures at downstream stations were found to be consistent with single phase results at matching local conditions. These comparisons are presented in detail in chapter 6 as part of the results.

5.4 Uncertainty Analysis

Composite uncertainties for the reduced data were evaluated using the basic approach recommended by Kline and McClintock (1953). In practice the required influence coefficients for each independent variable were calculated using as a basis the computer program prepared for the primary data reduction process outlined in the preceding sections. This was done by subjecting each input variable, in turn, to a slight perturbation from its measured value and recomputing the output. The required influence coefficients (partial derivatives) could then be approximated as finite differences.

The uncertainty analysis was performed for five representative points at widely varying conditions. To compare single-phase air-only results with correlation 3-9, the absolute accuracy of instrumentation was important. The uncertainty was estimated with absolute accuracy as the criterion. However in comparing single-phase and two-phase results at "matching local conditions," any uniform bias in measurements was not significant. For purposes of this comparison uncertainty was estimated using repeatability as the criterion.

For the single-phase results, the estimated uncertainty was ±3% for the Reynolds number, ±8% for the Nusselt number (absolute basis). For the comparison of two-phase with single-phase wall temperatures (relative basis), the uncertainty in the measured wall temperature was ±0.5K. The uncertainty in the interpolated single-phase wall temperatures used for comparison was ±6K for most of the tests, up to ±15K in two cases. The higher value arose because of a larger uncertainty associated with the water rotameter used in those two tests.

6. RESULTS AND DISCUSSION

Tests were conducted in series (section 4.2), beginning with air-only (preheated), zero-power input calibration tests, then adding test-section power input for single-phase tests, and finally adding various amounts of water for two-phase tests. Within a series, the air mass flow rate and temperature entering the atomizer were held constant. The calibration tests were used for determination of heat leaks as described in Appendix B. The single-phase and two-phase test results are presented and discussed here.

The reduced data are tabulated in chronological order in Appendix A for a total of 26 test runs (8 air-only runs and 18 with water injection). The data listed for a given run are based on the final data set observed for that run. Values of Nu_{VP} calculated from existing correlation 3-9 for single phase fully developed turbulent pipe flow are also listed for each run, including the two-phase tests with water injection.

Examination of Appendix A indicates that the Nu_{EXP} values for air-only tests ($M_W = 0$) appear to be quite consistent with Nu_{VP}. These air-only results will be compared in graphical form with correlation 3-9 and discussed further in section 6.1.

Nu_{EXP} for runs with liquid water present in the air stream ($M_W \neq 0$) was calculated using thermal conductivity of air evaluated at T_M (equation 5-8) and h defined in terms of T_M as characteristic fluid temperature (equation 5-1), just as in the

case of the air-only runs. Therefore, $Nu_{EXP}/Nu_{VP} = h_{EXP}/h_{VP}$, and overall consistency between Nu_{EXP} and Nu_{VP} should not be expected for these runs. That is indeed reflected by the tabulated values of Nu_{EXP}, many of which are very large compared with the corresponding values of Nu_{VP}, and some of which are negative. The negative values are a result of surface temperature (T_S) smaller than mixed-mean temperature (T_M), which is clearly possible for the nonequilibrium conditions resulting from the cold liquid water injected in the hot gas stream. However, in some of the cases with water injection values of Nu_{EXP} do become consisistent with Nu_{VP} at downstream stations. This may be interpreted as evidence that the liquid water has either all evaporated or nearly so and no longer significantly influences the heat transfer. This is discussed in more detail in section 6.5 where tube surface temperatures for cases with liquid water present in the air stream as it enters the tube are compared with single-phase cases at "matching local conditions."

A typical series of runs is presented in section 6.2 to show the effects of water injection on both wall temperatures and mixed-mean temperatures. To better understand the physics of the phenomena and aid in interpretation of the results, simple qualitative models are examined in sections 6.3 and 6.4. Finally, in section 6.5 surface temperatures for each of the 18 two-phase test runs are compared in graphical form to single-phase surface temperatures at "matching local conditions" (i.e., T_M, M_A, M_W, P_M, and q_{SM}). This isolates the effect of injected

water on surface temperature from its effect on mixed-mean fluid temperature. Three flow regimes are noted. The surface temperature comparisons and the major features of each flow regime are discussed in light of the qualitative models.

6.1 Single-phase Results vs Existing Correlation

Eight runs were made with air only, at various combinations of flow rate, inlet temperature, and heat flux. The data were reduced to the dimensionless parameters Nu, Re, Pr, Z/D. The Nusselt numbers are shown on figure 6-1. The first wall thermocouple location was in the developing-flow region. The data for this location are not shown, since the relevant correlation is valid only for fully-developed profiles.

For comparison with prior work, the central line on figure 6-1 represents correlation 3-7. As noted in section 3.3, this was recommended for fully developed flow of gas in a tube, with constant fluid properties. For valid comparison then, the experimental data were adjusted to constant property conditions using equation 3-4.[6]

The correlation line was calculated using the average Prandtl number of all points shown. The experimental Prandtl number of the data varied less than 2%. The other lines shown are 10% above and below the correlation. The data are consistent with the correlation line to within the estimated uncertainty intervals indicated at the bottom of the graph which represent

[6] Equations 3-7 and 3-4 were recommended by Kays and Crawford (1980), with n in 3-4 as given by 3-6.

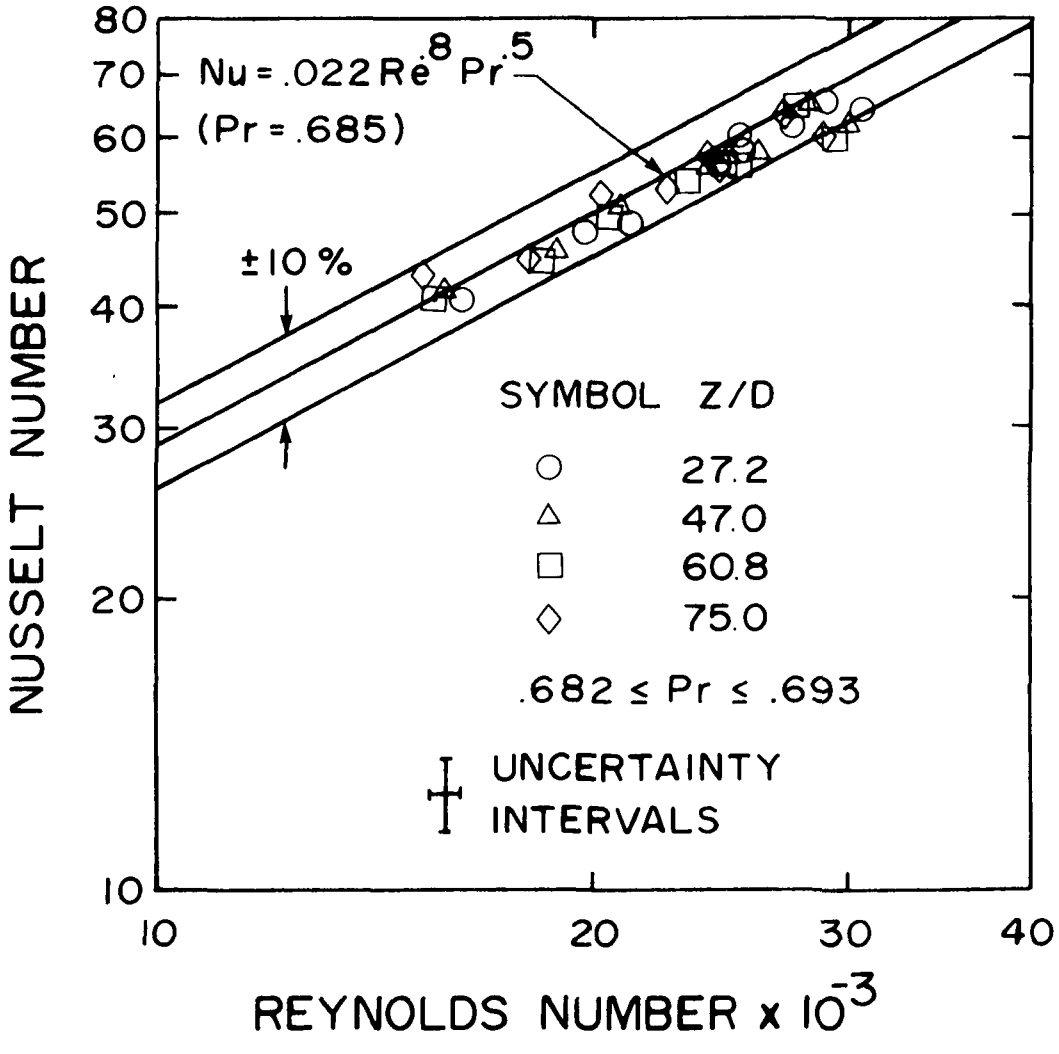

Figure 6-1 Air-only Results

±3% for Reynolds number and ±8% for Nusselt number. This level of agreement is consistent with that of other experimenters. Sleicher and Rousse (1975) compared several existing correlations with some 120 data points, and noted deviations up to 100%. The maximum deviation from their recommended equation was 18%, with an average of 4.2%. The present results are thus quite acceptable, especially considering the difficulties associated with heat transfer measurements for a very small diameter tube, and promote confidence in the experimental facility, instrumentation, and data reduction techniques.

6.2 Effects of Water Addition

Consider the measured wall temperature and calculated mixed-mean fluid temperature data in figure 6-2. A typical series of four test runs is shown, at various mass fractions of liquid. The upper set of lines (run 166) is data from an air-only run. Note that both wall and fluid temperatures rise linearly with distance as would be expected for a fully-developed flow with uniform heat flux. The fluid to wall temperature difference is large and positive. A development-length effect appears to influence the first wall temperature measurement.

The remaining sets of lines represent data from two-phase tests. The temperature of the air entering the atomizer was similar in all cases, but the mixed-mean fluid temperature is seen to drop significantly as water flow is increased. Note the effect is limited by saturation; the drop in inlet mixed-mean

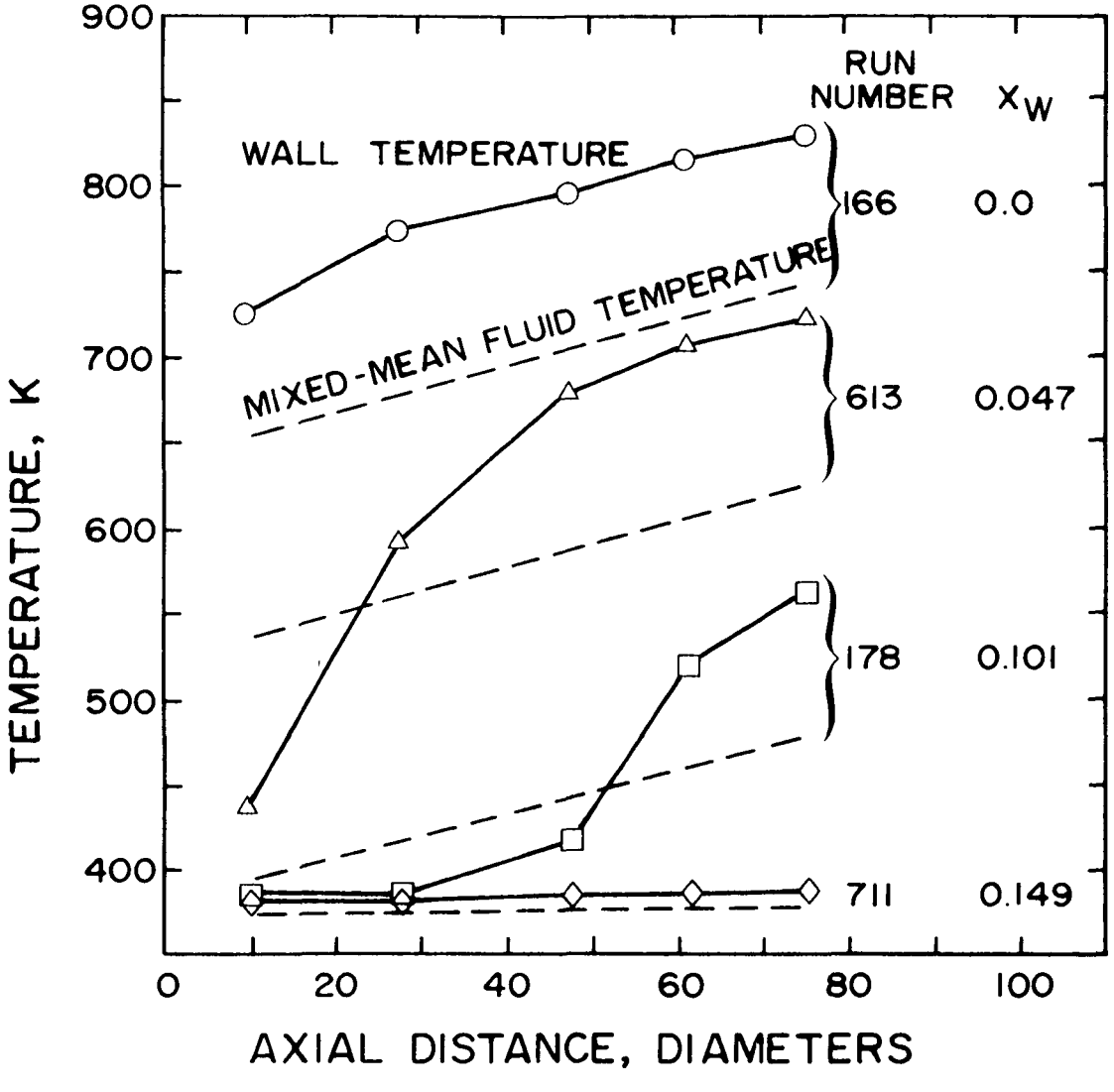

Figure 6-2 Representative Series

Wall Temperature ....Solid Line with Symbols
Mixed-mean Fluid Temperature.....Dashed Line

temperature is almost negligible as the mass fraction of water injected is increased from 10% to 15%. Note also that the slope of the mixed-mean temperature line is similar for all runs except at 15%. This indicates that the 5% and 10% mixtures would be all gas-phase if allowed to equilibrate adiabatically.

Now consider the wall temperature data. Near the outlet, wall temperatures in runs 613 and 178 behave similarly to the air-only run 166. This suggests the mixture is gas-phase, at least near the wall. At the inlet, the wall temperature behavior is quite different. In runs 613 and 178 the temperature is below the mixed-mean fluid temperature for some length. The uniform wall temperature behavior which first clearly appears near the inlet for run 178 at 10% water mass fraction extends all the way to the outlet for run 711 for which the mass fraction is 15%. These phenomena can be better understood by considering qualitatively in more detail the relevant idealized physical models from chapter 2.

6.3 Single-phase Idealized Model

Recall the models defined in section 2.1. Case 1 featured single-phase, two-component flow at the inlet to the heated section. Trends of temperature and liquid mass fraction variation are shown in figure 6-3. Average gas-phase (air + water vapor) temperature (T_G), average liquid temperature (T_ℓ), mixed-mean fluid temperature (T_M), and liquid mass fraction

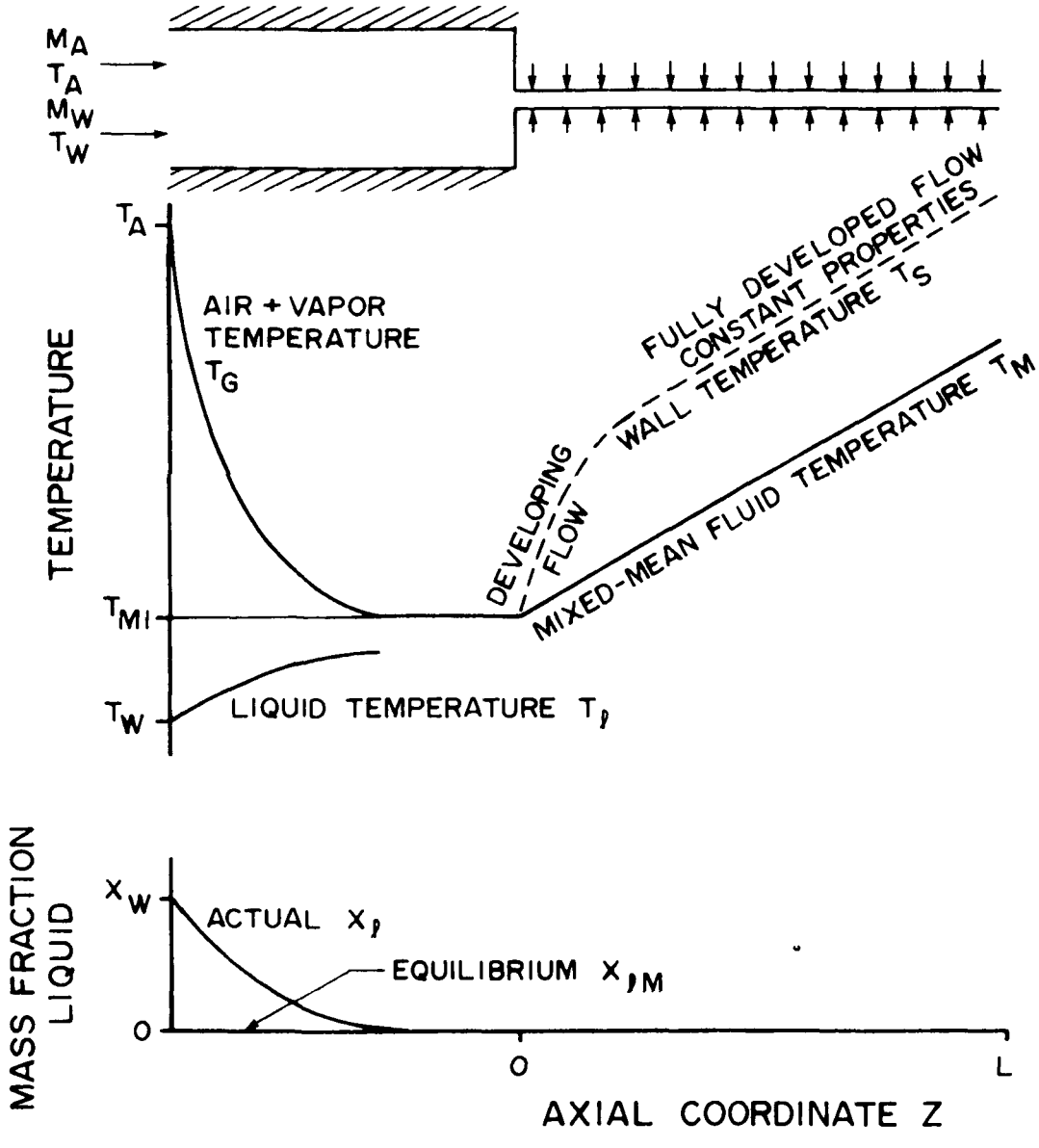

Figure 6-3 Idealized Model Case 1

Single-phase, Equilibrium

(X_ℓ) are shown as solid lines. Wall temperature (T_S) is shown as a dashed line.

With specified values of T_A, T_W, M_A, M_W, and P_M, the mixed-mean fluid temperature can be determined from the system of equations 5-5. T_M must be constant in the adiabatic mixing chamber. As the mixture traverses the uniformly heated section, its enthalpy increases linearly with distance. Assuming constant properties, the temperature (T_M) must also increase linearly. Since the mixture is all gas, this is also the average gas temperature (T_G). The main features of the model are the linearly increasing wall temperature and the relatively large, constant temperature difference beyond the developing-flow region.

Note the figure indicates that the gas in the mixing chamber cools rapidly while the liquid temperature increases only slightly. The last of the liquid evaporates well below the gas temperature. Assuming local equilibrium at the interface, the liquid will evaporate at the saturation temperature corresponding to the local vapor pressure. Heat transfer is usually limited by the gas-side resistance, so the liquid temperature is nearly uniform. Temperature and concentration gradients present in the gas mean its average temperature is above the interface temperature.

6.4 Two-phase Idealized Models

Consider the idealized physical models of two-phase, non-equilibrium flow presented in section 2.1 (cases 2 and 4). These are shown in figures 6-4 and 6-5, respectively, using the same format and symbols as in figure 6-3. Consider first figure 6-4. Recall that case 2 has identical conditions at the entrance to the mixing chamber as case 1. Thus, the behaviors of T_G, T_M, T_ℓ, and X_ℓ are identical for $Z \leq 0$. Since the heat flux and heated section length in cases 1 and 2 are identical, T_M is also identical for $0 < Z < L$. The differences are in T_G, T_S, T_ℓ, and X_ℓ in the region $0 < Z < L$. Two limiting case models of their behavior are shown in figure 6-4 similar to the two limiting cases defined in section 3.2, corresponding to annular and mist regimes.

First, if the flow is annular at $Z = 0$, heat transfer can occur only from the wall to liquid or from gas to liquid (neglecting radiation). But the evaporating water tends to prevent significant heat transfer from the gas to liquid. Thus, the gas is cooled only by mixing with the lower temperature vapor. This effect is small compared to the evaporative cooling which occurs in the mixing chamber, so the gas temperature is approximately constant. The liquid temperature may rise slightly, but most wall heat goes to vapor generation. The wall temperature is determined by the liquid properties, causing the temperature difference to be relatively small. The wall temperature is approximated by the dashed line labeled "liquid

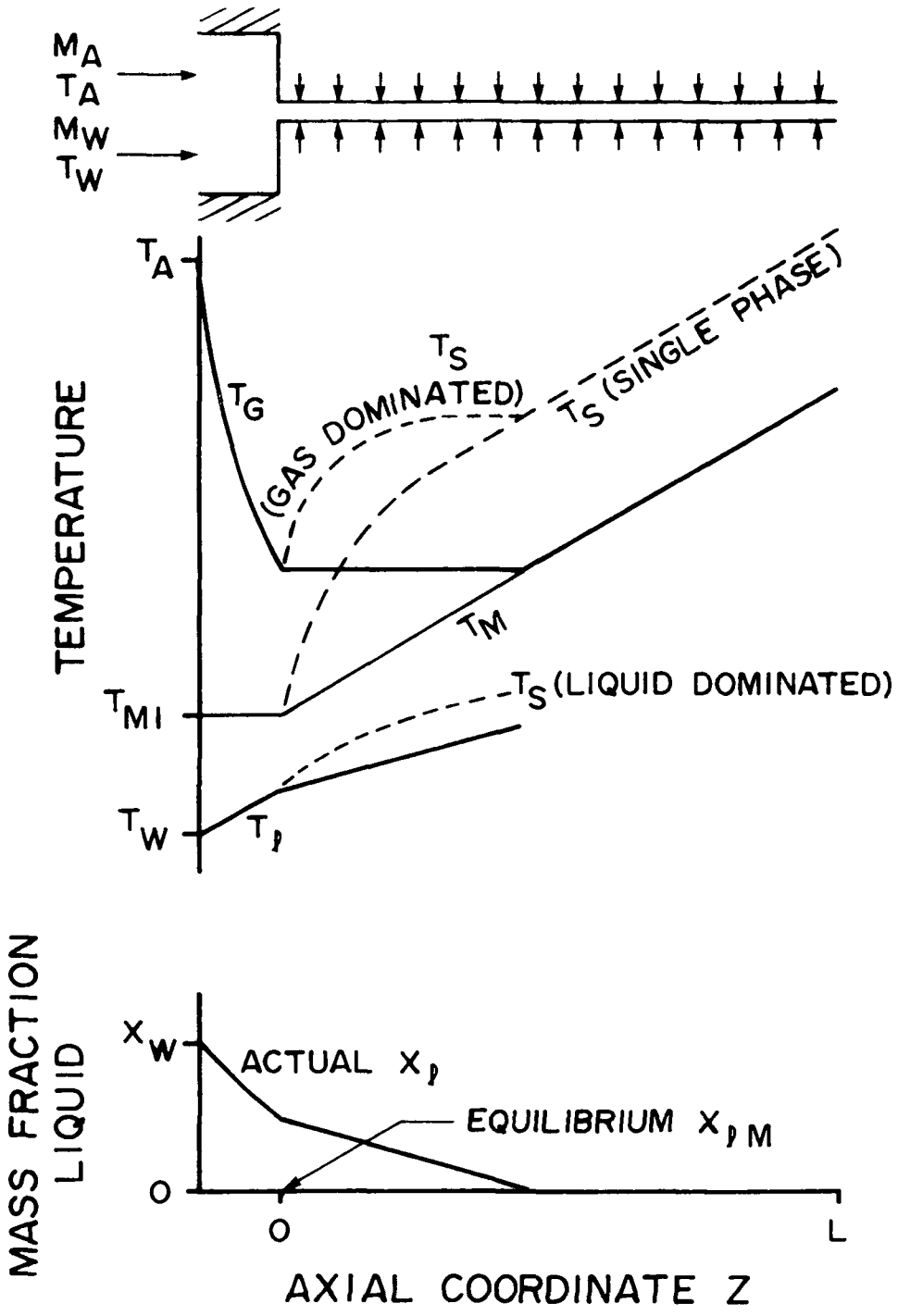

Figure 6-4 Idealized Model Case 2

Two Phase, Disequilibrium

dominated." This line ends when all liquid has evaporated, at which point the gas contacts the wall. Temperature then rises through some undefined transition to the line labeled "single-phase."

Second, if the liquid is in mist form at Z = 0, a different limiting case model might apply. Droplets in the main stream are subject to turbulent eddies and one might expect effective heat exchange with the gas.[7] Assuming perfect equilibrium between droplets and main-stream gas, one finds the specific heat of the mixture is very large. Thus, the average gas temperature remains almost constant until all the liquid evaporates, at which point the mixture becomes single-phase. Any droplets in the boundary layer would be exposed to less turbulence than droplets in the main stream, and slower heat exchange with the gas might be expected. Thus, the mixture in the boundary layer would tend to have a specific heat nearer that of the gas phase. If one neglects droplets impacting the wall (i.e. $\epsilon = 0$), the wall temperature is determined by gas properties. These result in a relatively large temperature difference, per the dashed line labeled "gas dominated." Note this meets the "single-phase" behavior as the liquid evaporates.

Case 4 behavior (figure 6-5) is virtually identical to case 2, except that the transition to "single-phase" behavior is delayed by the additional water.

[7] Rane and Yao (1981) treated dispersed droplets as distributed heat sinks in similar fashion.

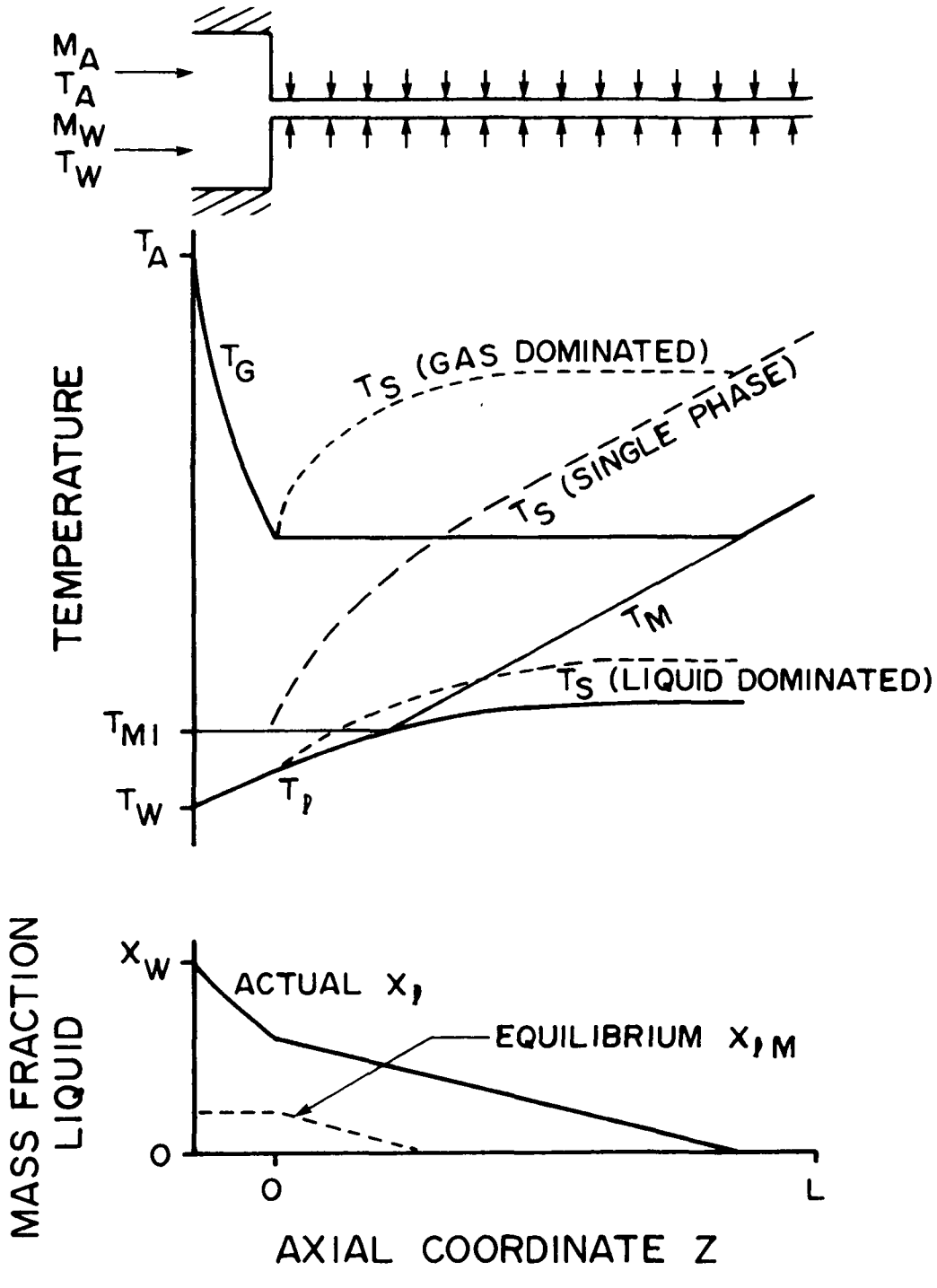

Figure 6-5 Idealized Model Case 4

Two Phase, Disequilibrium

The main features of the two-phase, non-equilibrium model behavior are:

- Low wall temperature in the "liquid dominated" region (possibly below T_M)
- High wall temperature in the "gas-dominated" region (overshoots "single-phase" T_S)
- Wall temperature eventually reaches "single-phase" after liquid evaporates
- Linear increase of wall temperature in "single-phase" region
- Undetermined behavior in the transition between "liquid dominated" and either "gas dominated" or "single-phase" regions.

Consider now the two-phase behavior on figure 6-2 in light of these models. Note the low wall temperature near the inlet suggested by the "liquid dominated" model is consistent with all two-phase runs. Also, the high temperature difference near the outlet in runs 613 and 178 is consistent with "single-phase" behavior. Clearly runs 613 and 178 show a transition between "liquid dominated" and "single-phase." Whether this transition follows the pattern suggested by the "gas-dominated" model is unclear. Key to this determination is whether the wall temperature ever overshoots the "single-phase" wall temperature which would occur at "matching local conditions."

6.5 Two-phase vs Single-phase Wall Temperatures

To compare with two-phase wall temperatures at "matching local conditions," single-phase wall temperatures computed using correlation 3-9 would be reasonably accurate. However,

figure 6-1 indicates that on average correlation 3-9 slightly overpredicts the single-phase data oobtained with the present test facility. Therefore, in order to make the comparison one which minimizes possible bias (however small) unique to the particular test facility, single-phase wall temperatures for the comparison at matching conditions were determined as follows. For each two-phase test, a single-phase air-only test with similar temperature levels was selected. The air-only test wall temperatures were then adjusted to conditions matching the two-phase conditions by assuming proportionality in the form of correlation 3-9; i.e., ignoring the particular value of the leading constant. This leads to

$$\frac{\{q_{SM}/[(T_S-T_M)K]\}_1}{\{q_{SM}/[(T_S-T_M)K]\}_2} = \frac{\{Pr^{.5}\ Re^{.8}(T_S/T_M)^n\}_1}{\{Pr^{.5}\ Re^{.8}(T_S/T_M)^n\}_2} \qquad 6\text{-}1$$

$$n = .3 - \{\log_{10}(T_S/T_M)\}^{1/4}$$

where subscript 1 refers to the conditions for the two-phase test it is desired to match and subscript 2 refers to the selected air-only test at similar temperature levels. This equation was solved iteratively for T_{S1}.

The calculations were made at each wall thermoucouple station, using local heat flux and fluid properties evaluated at the local pressure and mixed-mean temperature. The mixed-mean temperatures for the two-phase tests were determined from the systems of equations 5-4 or 5-5. Fluid properties for the equilibrium air/water mixture at the mixed-mean temperature were

evaluated neglecting the presence of the water component as discussed near the end of section 5.2.

Measured wall temperatures for the six series of two-phase test runs are plotted in figures 6-6 through 6-11, with each value compared to a single-phase wall temperature at "matching local conditions." Each figure includes three graphs with progressively increasing water mass fraction. Since the air flow rate was nominally constant, the total mass flow and Reynolds number changed. A solid line joins the circular symbols which represent the wall temperature measured for the two-phase test at the conditions listed. The relevant run number is listed first, followed by the number of the selected run on which the single-phase wall temperatures are based. A solid line also joins the triangular symbols which represent the single-phase wall temperatures. The remaining solid line represents the mixed-mean fluid temperature at which the wall temperatures are compared.

Note that in all cases the two-phase wall temperatures are well below the single-phase wall temperature near the inlet. Apparently all tests included an inlet region with annular flow. In cases with large mass fractions of water wall temperatures remained low and uniform, implying the annular flow region extended to the outlet. In cases with small mass fractions of water, downstream wall temperatures increased considerably. This implies a transition to mist or single-phase flow. In some cases the two-phase and single-phase wall temperatures merge to a common value, but within experimental uncertainty the two-phase

temperature never exceeds the single-phase value. The uncertainties in wall temperatures (section 5.4) were such that in most cases the uncertainty interval is approximately equivalent to or less than the data point symbol size used in the figures. Where the uncertainties exceed the symbol size, the intervals are indicated by a vertical bar attached to the data point symbol.

Three additional points should be made regarding these results. First, since there is no clear evidence of the wall temperature from any two-phase test overshooting the wall temperature for the single-phase case, it appears that the "gas-dominated" behavior as discussed in section 6.4 did not occur. (Only run 29 in figure 6-9 shows any tendency for the wall temperature from the two-phase test to exceed the value for the single phase case, but even there when experimental uncertainty is considered it can at most be concluded that the points merge.) Recall that the limiting case "gas-dominated" model neglected droplet/wall interaction effects and in the boundary layer neglected droplet/gas interaction. As Pedersen showed (1970), the droplet/wall interaction can be significant if the droplets wet the wall. The wall temperatures in the region being considered here were below the threshold value above which wetting does not occur (the Leidenfrost temperature). A model including some direct droplet/wall heat transfer contribution (along the lines of that used by Mastaniah and Ganic in 1981) may be more appropriate for these conditions.

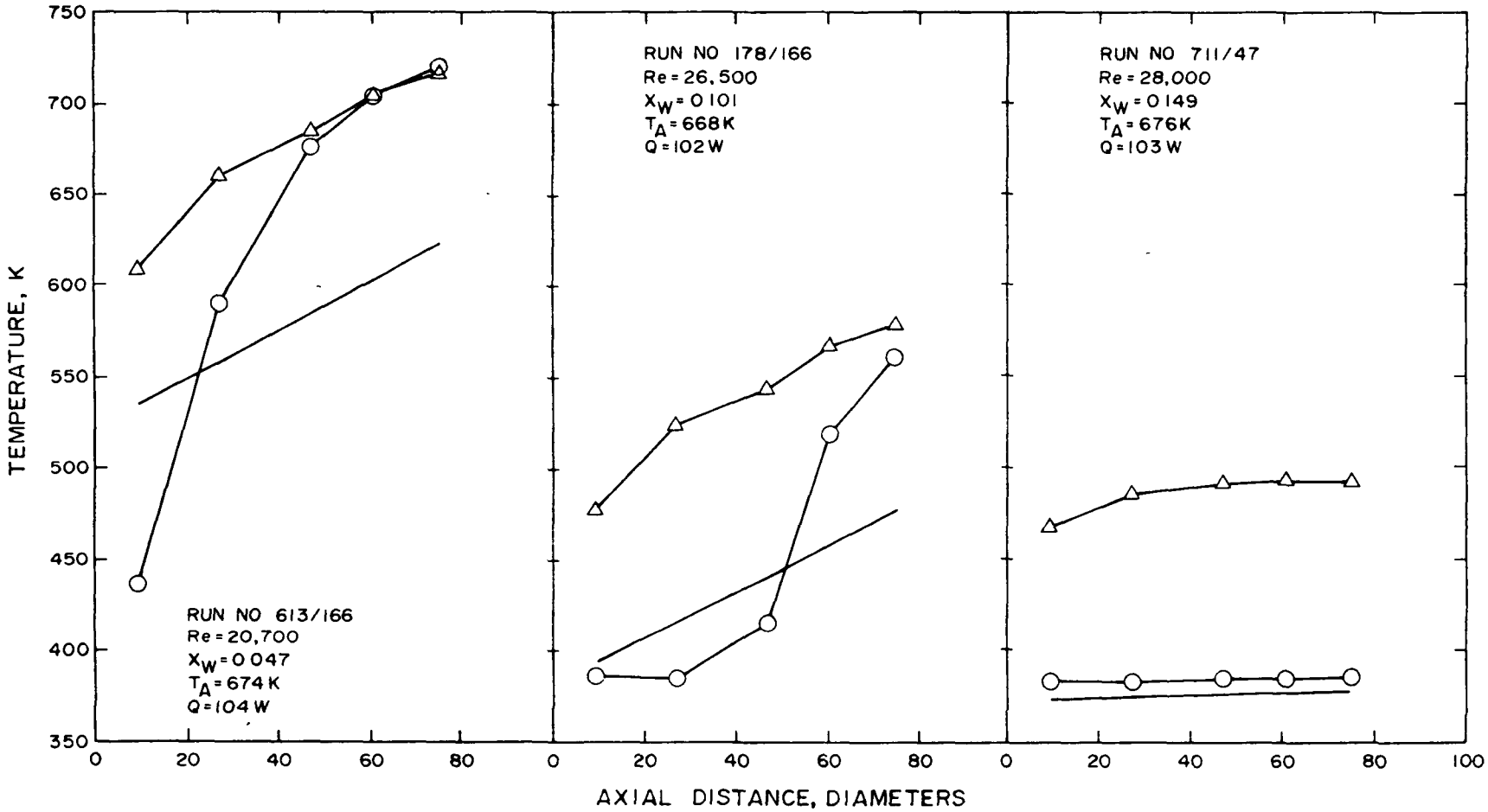

Figure 6-6 Wall Temperatures for Two-Phase Tests Compared with Single-Phase Values at "Local Matching Conditions"

○ Wall Temperature for Two-phase Test △ Single-phase Wall Temperature
—— Mixed-mean Fluid Temperature

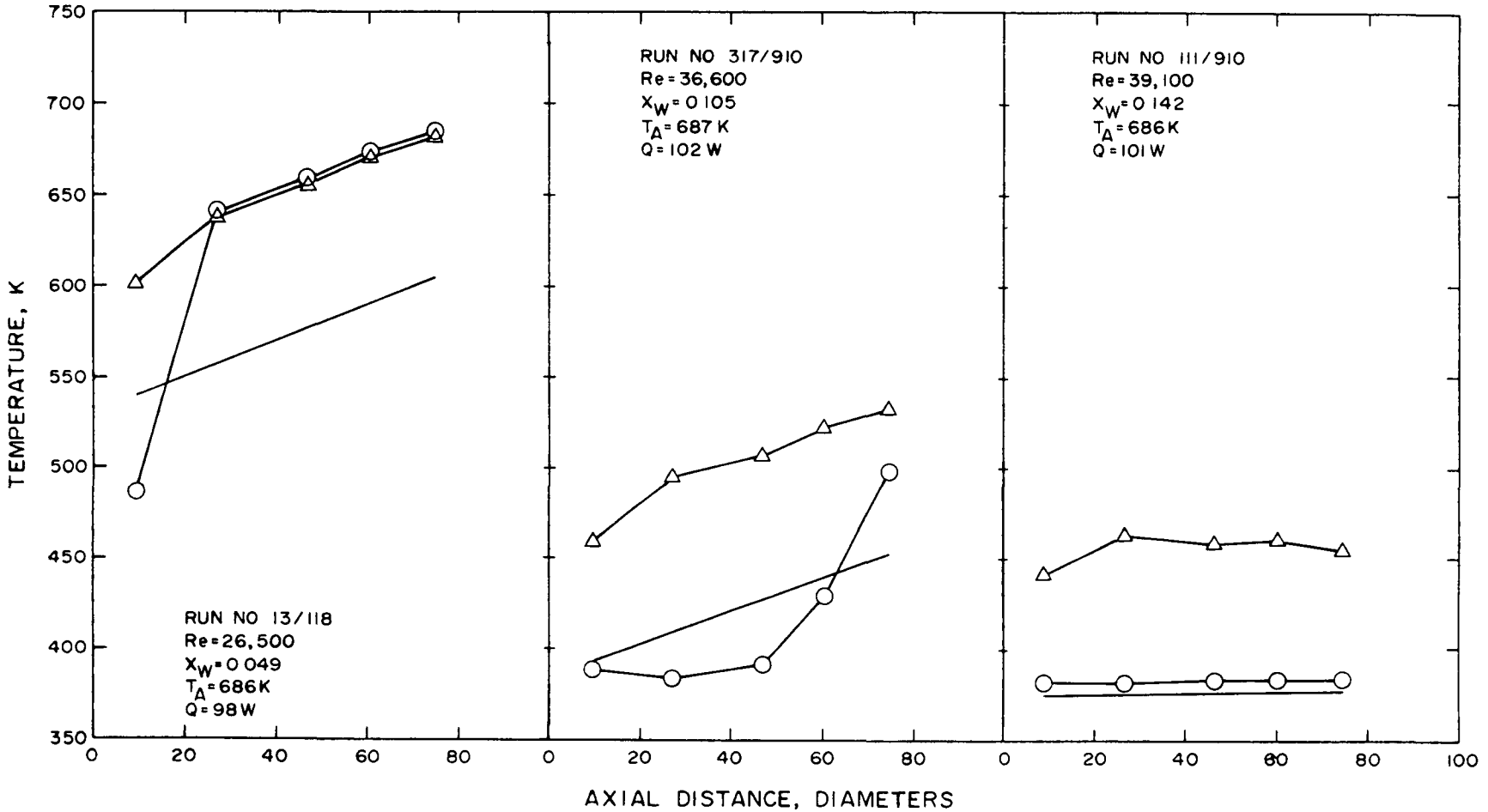

Figure 6-7 Wall Temperatures for Two-Phase Tests Compared with Single-Phase Values at "Local Matching Conditions"

○Wall Temperature for Two-phase Test △Single-phase Wall Temperature
—— Mixed-mean Fluid Temperature

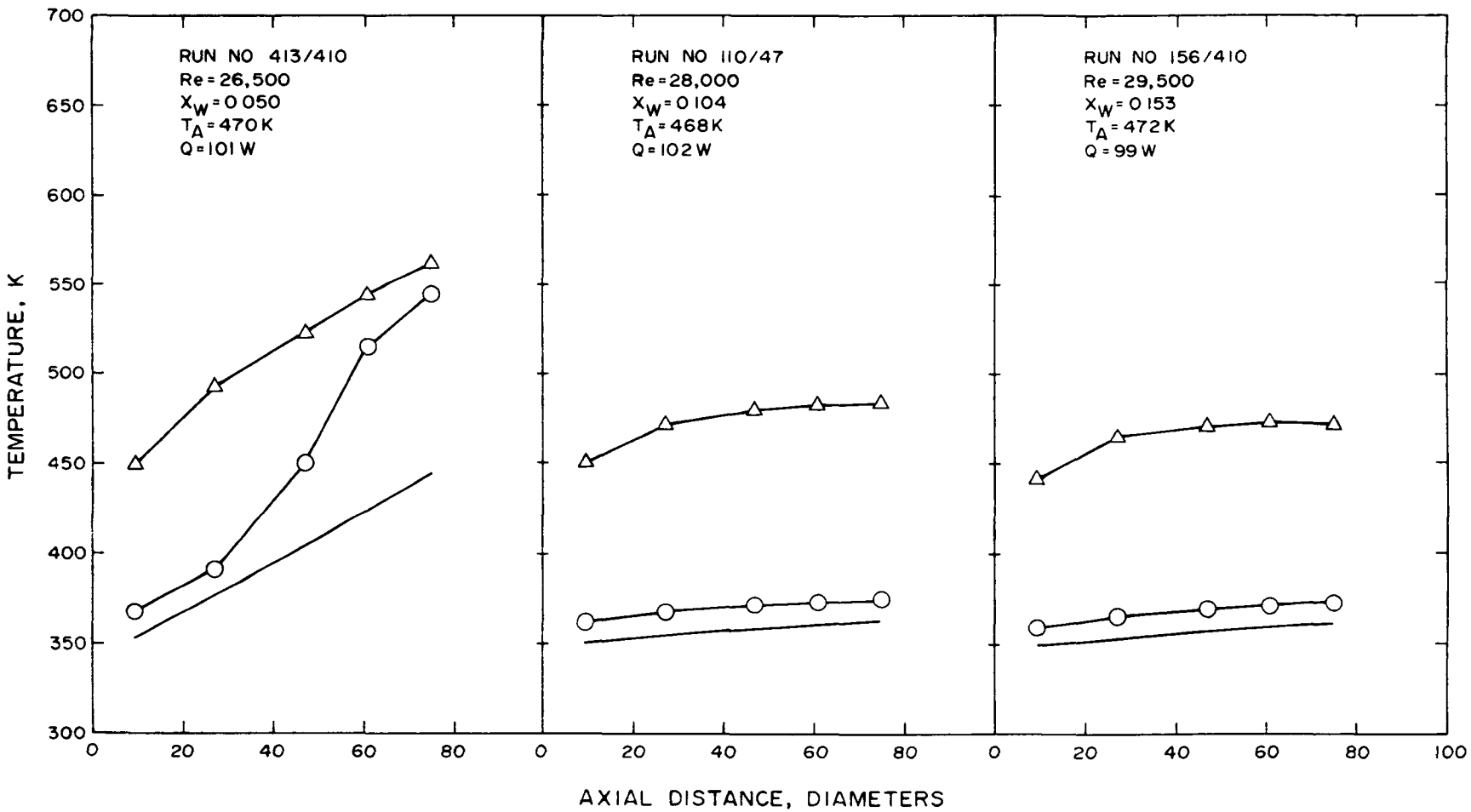

Figure 6-8 Wall Temperatures for Two-Phase Tests Compared with Single-Phase Values at "Local Matching Conditions"

○ Wall Temperature for Two-phase Test △ Single-phase Wall Temperature
—— Mixed-mean Fluid Temperature

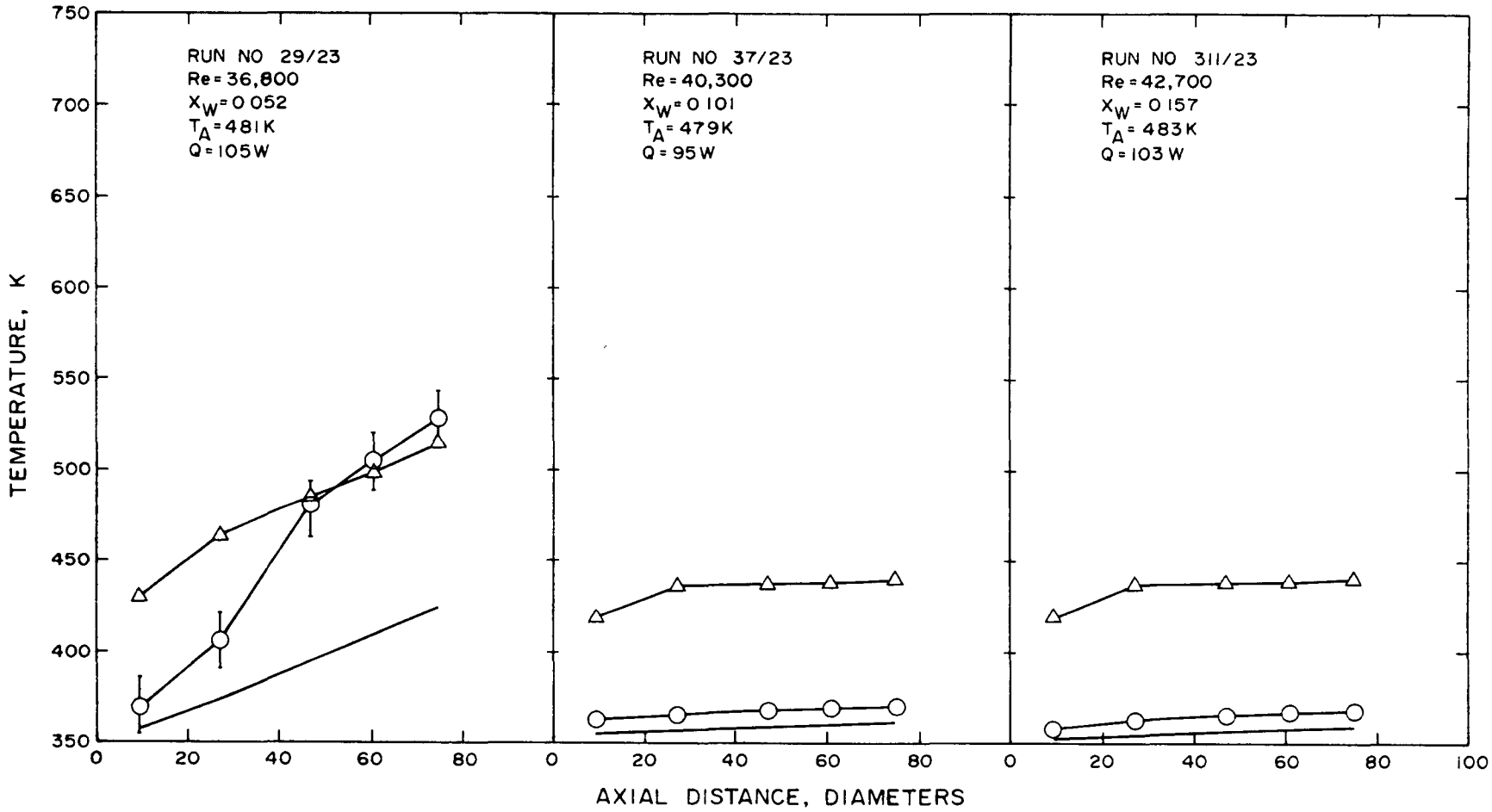

Figure 6-9 Wall Temperatures for Two-Phase Tests Compared with Single-Phase Values at "Local Matching Conditions"

○Wall Temperature for Two-phase Test △Single-phase Wall Temperature
—— Mixed-mean Fluid Temperature

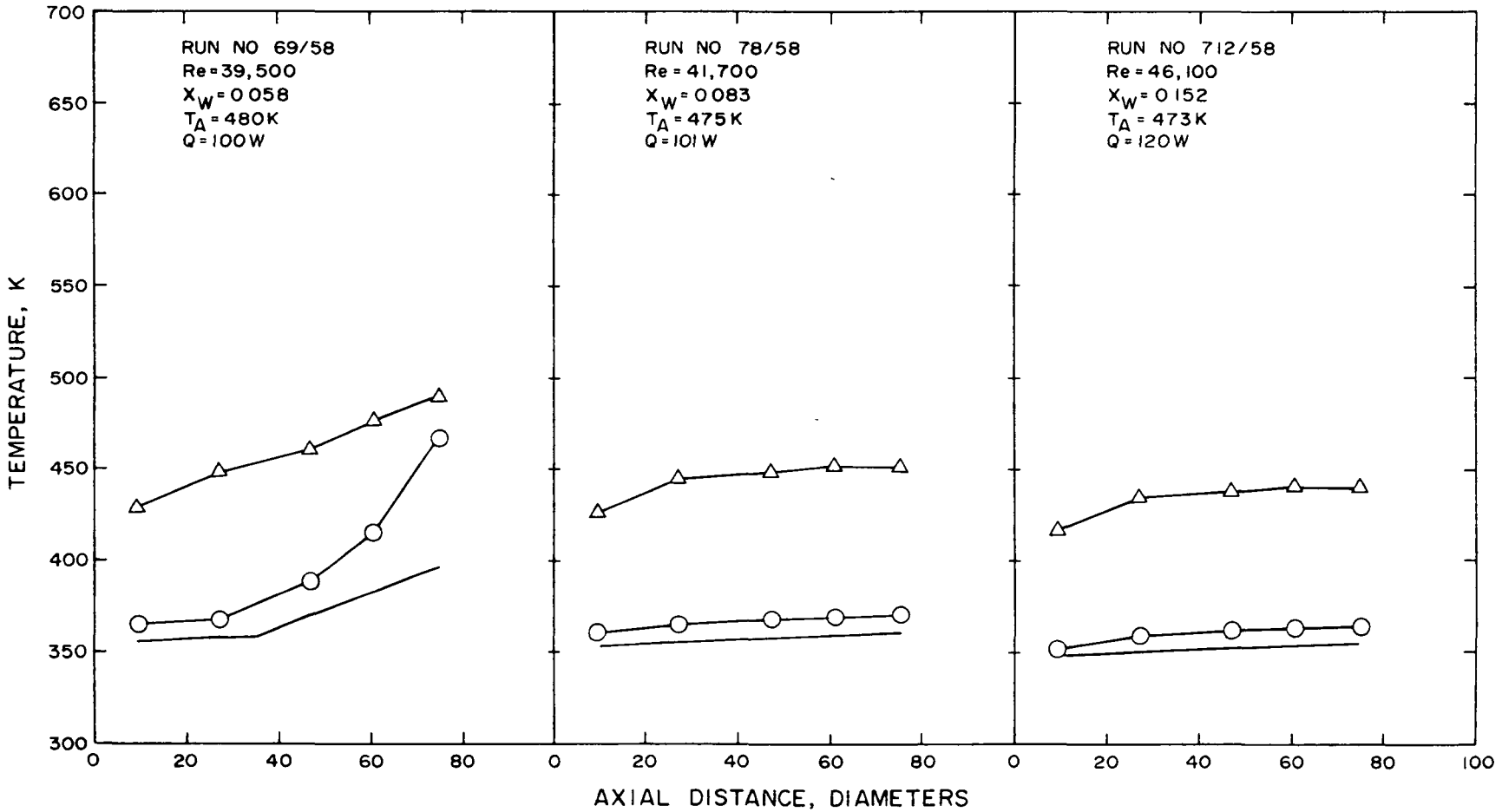

Figure 6-10 Wall Temperatures for Two-Phase Tests Compared with Single-Phase Values at "Local Matching Conditions"

○Wall Temperature for Two-phase Test △Single-phase Wall Temperature
——Mixed-mean Fluid Temperature

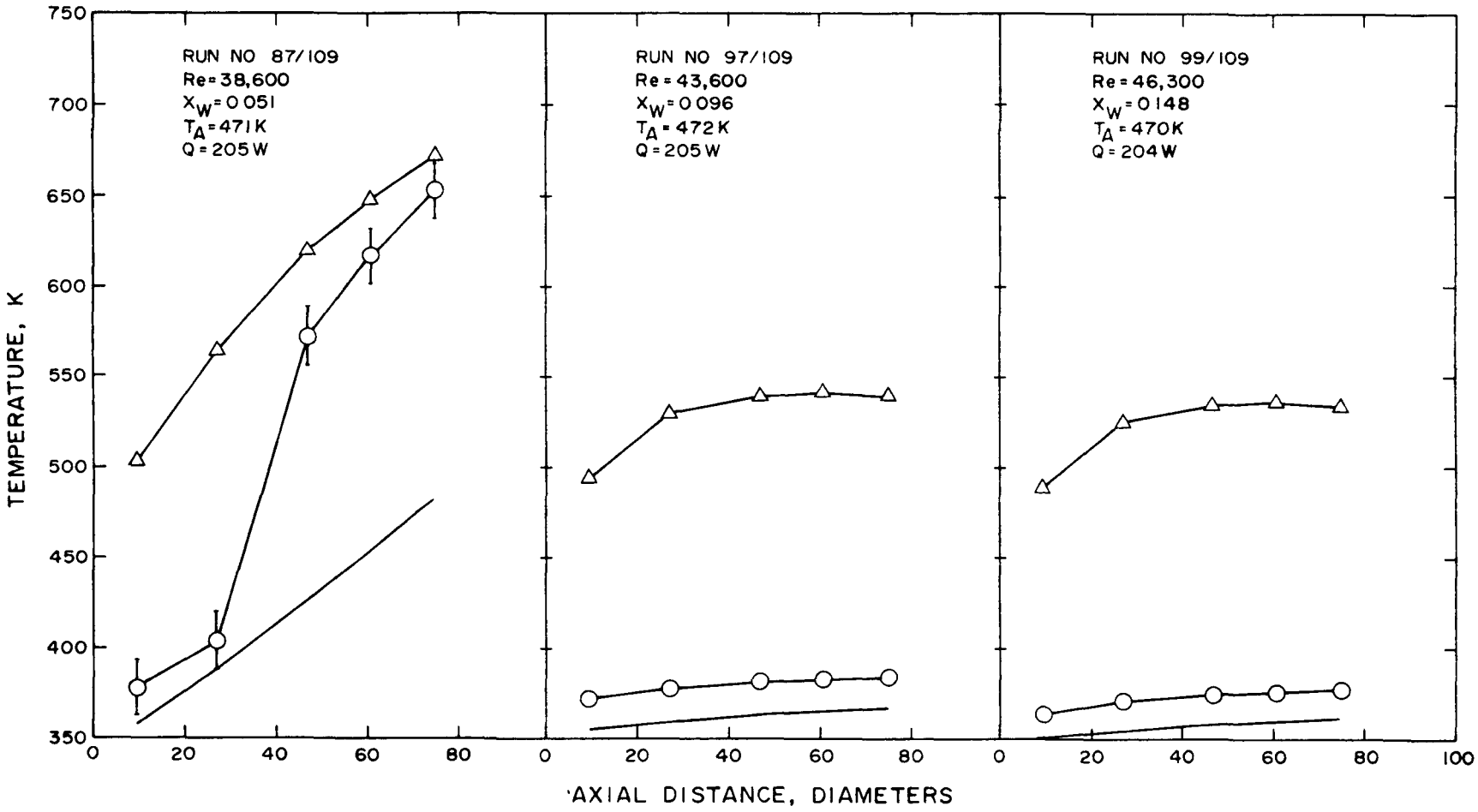

Figure 6-11 Wall Temperatures for Two-Phase Tests Compared with Single-Phase Values at "Local Matching Conditions"

○Wall Temperature for Two-phase Test △Single-phase Wall Temperature
—— Mixed-mean Fluid Temperature

Another possibility would be to allow for droplet influence on gas-phase temperature in the boundary layer. The "gas-dominated" model neglected any droplet influence (direct or indirect) on the wall heat transfer. If one assumes rapid heat transfer between droplets and gas, the specific heat increases about an order of magnitude. The resulting decrease in temperature difference relative to the "gas dominated" model may also be an explanation for the lack of any observation of "overshoot." The relative importance of the droplet/wall contact and droplet/gas interaction is not clear.

Second, note the contrast in the abrupt transition of run 13 in figure 6-7 with the more moderate change of run 317 in the same figure. Transitions on the remaining figures are all of the more moderate type, with the possible exception of run 87 on figure 6-11. Recall that Mori, et al. (1982) speculated some transitions occurred from annular directly to single-phase flow while others went through an intermediate mist regime. If the liquid film in figures 6-4 or 6-5 were to evaporate without any droplets present, a step change in wall temperature might be expected (neglecting axial conduction and boundary layer growth). Run 13 (figure 6-7) appears to approximate such behavior. With mist present, the droplets randomly impacting the wall might tend to smooth the transition as in run 317 and a number of others. The results suggest both types of transition occurred.

Finally, consider the direct transition from annular to single-phase regime. One would expect wall temperatures to

abruptly change from "liquid-dominated" to "single-phase," with some smoothing due to axial conduction and boundary layer growth. However, reconsidering the conditions just prior to the single-phase region suggests this might not be the case. If the liquid film is stable with no mist in the gas core, velocity and temperature near the wall are very low. The evaporating liquid will tend to carry its momentum and internal energy into the core flow, modifying the gas velocity and temperature profiles. The situation would be similar to flow in a porous-walled tube with blowing at the wall. Velocity and temperature would tend more to the parabolic laminar profile than the relatively flat turbulent profile. Immediately downstream of the dryout point, slow moving, relatively cool vapor would flow adjacent to the wall, acting like a very thick boundary layer (as opposed to the very thin wall region present in fully developed turbulent flow or immediately downstream of an entrance with a uniform profile). The turbulence in the gas core would rapidly thin the layer, but it is conceivable the wall temperature might overshoot the fully-developed, single-phase value for a short distance. Eventually the behavior would be asymptotic to the "single-phase" line.

As noted, run 13 suggests a direct transition to single-phase, with no mist region. However, the single-phase wall temperature is not exceeded. If the overshoot phenomena occurred, it may have decayed between thermocouple locations. Another possibility is that the point of liquid disappearance is unsteady. Rapid fluctuations of the dryout point would tend to

smooth out the transition, but would not cause any response in the thermocouples and therefore go undetected.

7. CONCLUDING REMARKS

This research demonstrates a mixture of hot, dry air and cold liquid water cools a hot surface more effectively than the same mixture introduced to the same surface after the liquid has evaporated completely and cooled the hot air. This is shown for turbulent flow in a small diameter tube, with uniform heat flux boundary condition, in both annular and mist flow regimes. The physical phenomena may be better understood by considering the flow regimes individually.

In the annular regime, liquid flows adjacent to the tube wall. The lower temperature, higher specific heat and thermal conductivity of the liquid, and the enthalpy of vaporization associated with the phase change would lead one to expect low wall temperatures. This was found to be the case.

In mist flow, the gas is in contact with the heated wall. This gas is hotter than it would be with initial equilibrium since all of the liquid has not yet evaporated, so one might expect higher wall temperatures. Also, the presence of the condensed phase in effect reduces the gas velocity relative to the initial equilibrium situation. Cold droplets impacting the wall would tend to offset these effects, whether or not wetting occurs. Further, the effective specific heat of the binary two-phase mixture is an order of magnitude greater than the gas alone. Therefore, whether the surface temperature which could be acheived by cooling with mist flow would be smaller than that

which could be acheived by cooling with the gas stream after complete evaporation of the liquid was not clear *a priori*.

The present results demonstrate the superior cooling effectiveness of the two-phase non-equilibrium mixture. However, for use in design/feasibility studies of contingency cooling of gas turbine blades a wider range of variables would have to be investigated. Of particular interest would be total pressure and wall temperature levels. The present tests were limited by the pressure level available from the laboratory compressor. Tests at higher wall temperature levels were planned, but not completed because of faster than anticipated deterioration of parts of the apparatus at the temperatures achieved.

It appears that the mist flow regime would be most desirable for gas turbine cooling. With sufficiently high wall temperatures wetting of hot components by the mist particles would not occur. This could prevent thermal shock failure. A number of the present tests appear to include regions of mist flow, but always following a region of annular flow. This may be unavoidable with internal flow and the uniform heat flux boundary condition used here. Goodyer and Waterston (1974) used a jet impingement geometry and observed heat transfer during what they interpreted as dry wall mist flow at surface temperatures of about 900K. However, in their tests both the air and the liquid water were introduced at nominally room temperature levels. Further investigation using this geometry may hold some promise.

As applied to contingency cooling of gas turbine blades, direct liquid injection could provide a given level of transient power operation with less water than required for evaporative cooling. The demonstrated benefits of improved heat transfer are not obtainable without difficulty. Clearly there is a danger of thermal shock failure if wetting occurs. Also, delivery of cold liquid to the blade cooling passages is not a simple matter. In an engine the water delivery passages would be at elevated temperatures when water flow started. The liquid may begin boiling on contact with the passages. Delivery of liquid to the critical blade surfaces would be delayed until the passages cooled sufficiently. Thus, additional cooling capability required for contingency power operation would not be immediately available.

In summary, the technique which motivated the present investigation shows promise, but is fraught with hazards. Further investigation is needed to determine if the hazards can be avoided and the benefits realized. Research is also needed to understand the relative importance of droplet/wall interaction and droplet/gas interaction in reducing wall temperatures or providing higher heat rates at a given wall temperature for cooling with air/water mist flows where the gas temperature is substantially above the liquid temperature.

REFERENCES

Collier, J.G. (1980): Convective Boiling and Condensation, McGraw Hill Book Company, London.

Dombrowski, N., and G. Munday (1968): "Spray Drying," Biochemical and Biological Engineering Science, vol. 2, ed. N. Blakebrough, Academic Press, London, pp. 211-320.

Dutton, R., and E.C. Lee (1959): "Surface Temperature Measurement of Current-Carrying Objects," Instrument Society of America Journal, vol. 6, no. 12, pp. 49-51.

Fiszdon, J.K. (1979): "Melting of Powder Grains in a Plasma Flame ," International Journal of Heat and Mass Transfer, vol. 22, no. 5, pp. 749-761.

Freche, J.C., and R.O. Hickel, (1955): "Turbojet Engine Investigation of Effect of Thermal Shock Induced by External Water-Spray Cooling on Turbine Blades of Five High-Temperature Alloys," NACA RM E55J17.

Goodyer, M.J., and R.M. Waterston (1974): "Mist Cooled Turbines," Heat and Fluid Flow in Steam and Gas Turbine Power Plants, Conference Publication 3, Institution of Mechanical Engineers, London.

Harpole, G.M. (1981): "Droplet Evaporation in High Temperature Environments," ASME Journal of Heat Transfer, vol. 103, no. 1, pp. 86-91.

Heyt, J.W., and P.S. Larsen (1971): "Heat Transfer to Binary Mist Flow," International Journal of Heat and Mass Transfer, vol. 14, no. 9, pp. 1395-1405.

Hishida, K., M. Maeda, and S. Ikai (1980): "Heat Transfer from a Flat Plate in Two-Component Mist Flow," ASME Journal of Heat Transfer, vol. 102, no. 7, pp. 513-518.

-----,-----, and ----- (1982): "Experimental Study on Heat Transfer in Binary Mist Flow (Effect of Incidence Angles of a Plate)," Heat Transfer - Japanese Research, vol. 10, no. 4, Trans. ed. G.A. Greene, pp. 71-87. Translated from Transactions of the J.S.M.E., 48; 428, pp. 758-766 (1982-4).

Kays, W.M., and M.E. Crawford (1980): Convective Heat and Mass Transfer, 2nd edition, McGraw Hill Book Company, New York.

Kline, S.J., and F.A. McKlintock (1953): "Describing Uncertainties in Single Sample Experiments," Mechanical Engineering, vol. 75, no.1, pp. 3-8.

Kutateladze, S.S., and Y.L. Sorokin (1969): "Hydrodynamic Stability of Vapor-Liquid Systems," Problems of Heat Transfer and Hydraulics of Two-Phase Media, Trans. ed. J.G. Collier, Pergamon Press, London, pp. 385-395.

Kuwahara, H., W. Nakayama, and Y. Mori (1982): "Heat Transfer from the Heated Cylinders with Various Surfaces in Air/Water Mist Flows," Heat Transfer -Japanese Research, vol. 10, no. 2, Trans. ed. G.A. Greene, pp. 1-19. Translated from Transactions of the J.S.M.E., 47; 414, pp. 326-335 (1981).

Liu, B.Y.H., and K.W. Lee (1977): "An Aerosol Generator of High Stability," Journal of the American Industrial Hygiene Association, vol. 36, no. 12, pp. 861-865.

Lorenzetto, G.E. (1976): Influence of Liquid Properties on Plain-Jet Airblast Atomization, PhD dissertation, Cranfield Institute of Technology.

Mastanaiah, K., and E.N. Ganic (1981): "Heat Transfer in Two-Component Dispersed Flow," ASME Journal of Heat Transfer, vol. 103, no. 2 pp. 300-306.

Meyer, C.A., R.B. McClintock, G.J. Silvestri, and R.C. Spencer (1977): ASME Steam Tables, 3rd edition, American Society of Mechanical Engineers , New York.

Miura, K., T. Miura, and S. Ohtani (1977): "Heat and Mass Transfer to and from Droplets," American Institute of Chemical Engineers Symposium Series, vol. 73, no. 163, pp. 95-102, AIChE, New York.

Mori, Y., K. Hijikata, and T. Yasunaga (1982): "Mist Cooling of Very Hot Tubules with Reference to Through- Hole Cooling of Gas Turbine Blades," International Journal of Heat and Mass Transfer, vol. 25, no. 9, pp. 1271-1278.

Peckner, D., and I.M. Bernstein (1977): Handbook of Stainless Steel, McGraw Hill Book Company, New York.

Pedersen, C.O. (1970): "An Experimental Study of the Dynamic Behavior and Heat Transfer Characteristics of Water Droplets Impinging upon a Heated Surface," International Journal of Heat and Mass Transfer, vol. 13, no. 2, pp. 369-381.

Rane, A.G., and S.C. Yao (1981): "Convective Heat Transfer to Turbulent Droplet Flow in Circular Tubes," ASME Journal of Heat Transfer, vol. 103, no. 4, pp. 679-684.

Ranz, W.E., and W.R. Marshall,Jr. (1952): "Evaporation from Drops ," Chemical Engineering Progress, vol. 48, no.3, pp. 141-146, no. 4, pp. 173-180.

Reynolds, W.C., and H.C. Perkins (1977): Engineering Thermodynamics, McGraw Hill Book Company, New York.

Richards, D.R. and L.W. Florschuetz (1983): Forced Convection Heat Transfer to Air/Water Vapor Mixtures, NASA Contractor Report 3769, Arizona State University, Tempe.

Rohsenow, W.M., and H. Choi (1961): Heat, Mass, and Momentum Transfer, Prentice-Hall, Englewood Cliffs, New Jersey.

Shapiro, A.H. (1953): Compressible Fluid Flow, vol. 1, Ronald Press Company, New York.

Sleicher, C.A., and M.W. Rouse (1975): "A Convenient Correlation for Heat Transfer to Constant and Variable Property Fluids in Turbulent Pipe Flow," International Journal of Heat and Mass Transfer, vol. 18, no. 5, pp. 677-683.

Van Fossen, G.J. (1983): "The Feasibility of Water Injection into the Turbine Coolant to Permit Gas Turbine Contingency Power for Helicopter Application," NASA report TM-83043, presented at 28th International Gas Turbine Conference, ASME, Phoenix, AZ.

Vasserman, A.A., Ya.Z. Kazavchinskii, and V.A. Rabinovich (1971): Thermophysical Properties of Air and Air Components, ed. A.M. Zhuravlev, Trans. Ch. Nishenbaum, Trans. ed. D. Slutzkin, Israel Program for Scientific Translations, Jerusalem.

Viannay, S., J. Joseph, and G. Dayan (1978): "Echanges Thermiques Entre une Surface Portee a Haute Temperature et un Melange d'Air et d'Eau Pulverisee Impactant Normalement" Proceedings 6th International Heat Transfer Conference, Toronto, vol. 4, pp. 97-100.

Appendix A---Reduced Data Tabulation

The following tables list the significant heat transfer related data from the final data set of each run. The runs are presented in chronological order. The nomenclature in the tables is consistent with that of the text. The values of air and water temperature, flow rate, and mixture pressure listed at the top of each table correspond to measured values within the atomizer. The values within the table are those measured or calculated at the stations where tube wall thermocouples were installed (see figure 5-1).

Run 23

P_M: 704 kPa T_A: 484.7 K M_A: 0.964 g/sec
T_W: N/A M_W: 0.0 mg/sec

	T5	T6	T7	T8	T9	Avg
Z (mm)	15	43	75	97	120	75
Z (dia)	9.4	27.2	47.0	60.8	75.0	46.9
T_M (K)	478.0	495.5	515.1	528.8	543.0	515.5
T_S (K)	540.6	572.5	590.9	603.7	618.2	585.0
Pr	0.685	0.684	0.683	0.683	0.683	0.683
Re	29,500	28,800	28,000	27,600	27,100	28,000
Nu_{VP}	66.6	65.4	64.1	63.2	62.4	64.1
Nu_{EXP}	79.5	63.7	63.2	63.0	61.8	68.8
q_{SM} (kW/m²)	121.7	123.3	124.3	125.0	125.7	124.0

Run 29

P_M: 704 kPa T_A: 481.2 K M_A: 0.924 g/sec
T_W: 361.5 K M_W: 51.2 mg/sec

	T5	T6	T7	T8	T9	Avg
Z (mm)	15	43	75	97	120	75
Z (dia)	9.4	27.2	47.0	60.8	75.0	46.9
T_M (K)	357.3	374.0	394.5	409.1	424.3	395.7
$X_{\ell M}$ (%)	0.1	0.0	0.0	0.0	0.0	0.0
T_S (K)	369.4	406.6	481.2	505.4	528.5	463.5
Pr	0.695	0.693	0.691	0.690	0.689	0.691
Re	36,700	35,500	34,100	33,300	32,400	34,100
Nu_{VP}	77.8	75.9	73.7	72.3	70.9	73.6
Nu_{EXP}	561.1	203.4	75.8	67.0	60.8	---
q_{SM} (kW/m²)	130.1	132.5	137.4	138.9	140.4	136.2

Run 37

P_M: 704 kPa T_A: 479.5 K M_A: 0.955 g/sec
T_W: 327.6 K M_W: 107.2 mg/sec

	T5	T6	T7	T8	T9	Avg
Z (mm)	15	43	75	97	120	75
Z (dia)	9.4	27.2	47.0	60.8	75.0	46.9
T_M (K)	354.7	356.9	358.9	360.1	361.2	358.9
$X_{\ell M}$ (%)	5.7	5.1	4.4	3.9	3.3	4.4
T_S (K)	363.2	366.2	368.5	369.8	370.9	367.5
Pr	0.695	0.695	0.695	0.695	0.695	0.695
Re	40,200	40,000	39,900	39,800	39,700	39,900
Nu_{VP}	84.4	84.1	83.9	83.7	83.6	83.9
Nu_{EXP}	765.4	694.0	670.0	664.7	662.1	---
q_{SM} (kW/m²)	124.3	124.5	124.7	124.8	124.8	124.6

Run 311

P_M: 686 kPa T_A: 482.9 K M_A: 0.944 g/sec
T_W: 317.6 K M_W: 176.4 mg/sec

	T5	T6	T7	T8	T9	Avg
Z (mm)	15	43	75	97	120	75
Z (dia)	9.4	27.2	47.0	60.8	75.0	46.9
T_M (K)	352.4	354.8	356.9	358.2	359.3	356.9
$X_{\ell M}$ (%)	11.9	11.3	10.6	10.1	9.6	10.6
T_S (K)	358.4	363.5	366.4	367.6	368.7	364.9
Pr	0.696	0.695	0.695	0.695	0.695	0.695
Re	42,600	42,400	42,200	42,100	42,000	42,200
Nu_{VP}	88.1	87.8	87.6	87.4	87.3	87.6
Nu_{EXP}	1174.9	802.4	741.1	747.2	743.5	---
q_{SM} (kW/m²)	134.3	134.7	134.9	135.0	135.1	134.8

Run 87

P_M: 707 kPa T_A: 471.4 K M_A: 0.967 g/sec
T_W: 348.6 K M_W: 52.3 mg/sec

	T5	T6	T7	T8	T9	Avg
Z (mm)	15	43	75	97	120	75
Z (dia)	9.4	27.2	47.0	60.8	75.0	46.9
T_M (K)	356.7	388.2	426.1	453.8	483.0	430.9
$X_{\ell M}$ (%)	0.05	0.0	0.0	0.0	0.0	0.0
T_S (K)	377.9	404.2	571.7	617.2	653.4	533.2
Pr	0.695	0.692	0.689	0.686	0.685	0.688
Re	38,400	36,100	33,800	32,300	31,000	33,500
Nu_{VP}	74.6	72.0	68.4	66.5	64.7	68.3
Nu_{EXP}	604.0	755.1	84.1	72.9	67.6	---
q_{SM} (kW/m²)	245.8	249.4	272.6	278.9	283.9	267.3

Run 97

P_M: 690 kPa T_A: 471.9 K M_A: 1.036 g/sec
T_W: 329.2 K M_W: 110.6 mg/sec

	T5	T6	T7	T8	T9	Avg
Z (mm)	15	43	75	97	120	75
Z (dia)	9.4	27.2	47.0	60.8	75.0	46.9
T_M (K)	354.8	359.2	363.1	365.3	367.2	363.1
$X_{\ell M}$ (%)	5.1	3.9	2.6	1.6	0.52	2.6
T_S (K)	372.2	378.1	381.6	382.8	384.4	379.2
Pr	0.695	0.695	0.695	0.694	0.694	0.695
Re	43,400	43,000	42,700	42,500	42,300	42,700
Nu_{VP}	82.8	82.4	82.0	81.8	81.6	82.0
Nu_{EXP}	775.6	706.8	720.2	757.0	770.1	---
q_{SM} (kW/m²)	258.5	259.4	259.9	260.0	260.3	259.5

Run 99

P_M: 617 kPa T_A: 470.2 K M_A: 1.027 g/sec
T_W: 321.3 K M_W: 177.8 mg/sec

	T5	T6	T7	T8	T9	Avg
Z (mm)	15	43	75	97	120	75
Z (dia)	9.4	27.2	47.0	60.8	75.0	46.9
T_M (K)	350.4	354.6	358.0	359.8	361.3	358.0
$X_{\ell M}$ (%)	10.7	9.6	8.3	7.3	6.2	8.3
T_S (K)	363.8	371.3	375.1	376.3	377.7	372.4
Pr	0.696	0.696	0.695	0.695	0.695	0.695
Re	46,000	45,600	45,300	45,100	45,000	45,300
Nu_{VP}	86.7	86.2	85.9	85.7	85.6	85.9
Nu_{EXP}	1054.6	841.0	820.3	848.7	844.0	---
q_{SM} (kW/m²)	267.3	268.4	269.0	269.2	269.5	268.6

Run 109

P_M: 617 kPa T_A: 483.7 K M_A: 0.951 g/sec
T_W: N/A M_W: 0.0 mg/sec

	T5	T6	T7	T8	T9	Avg
Z (mm)	15	43	75	97	120	75
Z (dia)	9.4	27.2	47.0	60.8	75.0	46.9
T_M (K)	486.9	523.4	564.9	594.0	624.3	567.4
T_S (K)	627.5	695.2	741.2	769.7	795.4	725.2
Pr	0.684	0.683	0.682	0.683	0.683	0.682
Re	28,800	27,400	26,000	25,200	24,400	26,000
Nu_{VP}	61.7	59.7	57.7	56.5	55.3	57.7
Nu_{EXP}	71.4	57.0	53.5	52.3	52.4	59.1
q_{SM} (kW/m²)	249.0	257.1	262.7	266.1	269.2	260.8

Run 410

P_M: 618 kPa T_A: 476.5 K M_A: 0.661 g/sec
T_W: N/A M_W: 0.0 mg/sec

	T5	T6	T7	T8	T9	Avg
Z (mm)	15	43	75	97	120	75
Z (dia)	9.4	27.2	47.0	60.8	75.0	46.9
T_M (K)	470.7	496.4	525.3	545.5	566.6	526.3
T_S (K)	560.3	605.0	635.1	655.0	672.9	625.5
Pr	0.685	0.684	0.683	0.683	0.682	0.683
Re	20,400	19,700	19,000	18,500	18,000	19,000
Nu_{VP}	48.7	47.5	46.2	45.3	44.5	46.1
Nu_{EXP}	56.5	45.5	43.6	42.8	43.1	48.0
q_{SM} (kW/m²)	122.2	124.5	126.1	127.2	128.1	125.6

Run 413

P_M: 617 kPa T_A: 470.2 K M_A: 0.661 g/sec
T_W: 362.1 K M_W: 34.7 mg/sec

	T5	T6	T7	T8	T9	Avg
Z (mm)	15	43	75	97	120	75
Z (dia)	9.4	27.2	47.0	60.8	75.0	46.9
T_M (K)	353.2	377.1	404.5	424.0	444.6	406.5
$X_{\ell M}$ (%)	0.01	0.0	0.0	0.0	0.0	0.0
T_S (K)	368.2	392.0	450.6	515.5	545.3	461.7
Pr	0.696	0.693	0.691	0.689	0.687	0.690
Re	26,400	25,200	23,900	23,200	22,400	23,900
Nu_{VP}	58.5	56.6	54.5	53.2	51.9	54.4
Nu_{EXP}	435.1	418.9	132.1	66.0	58.5	---
q_{SM} (kW/m²)	124.6	126.1	129.8	133.8	135.7	130.5

Run 156

P_M: 618 kPa T_A: 471.7 K M_A: 0.651 g/sec
T_W: 325.2 K M_W: 117.5 mg/sec

	T5	T6	T7	T8	T9	Avg
Z (mm)	15	43	75	97	120	75
Z (dia)	9.4	27.2	47.0	60.8	75.0	46.9
T_M (K)	349.6	353.5	357.2	359.5	361.5	357.2
$X_{\ell M}$ (%)	11.5	10.7	9.7	9.1	8.3	9.7
T_S (K)	359.3	366.0	369.7	371.6	373.3	367.8
Pr	0.696	0.696	0.695	0.695	0.695	0.695
Re	29,400	29,200	29,000	28,800	28,700	29,000
Nu_{VP}	63.9	63.6	63.2	63.0	62.9	63.2
Nu_{EXP}	705.8	547.8	542.5	554.6	569.1	---
q_{SM} (kW/m²)	129.4	129.9	130.1	130.2	130.4	130.0

Run 166

P_M: 618 kPa T_A: 689.5 K M_A: .665 g/sec
T_W: N/A M_W: 0.0 mg/sec

	T5	T6	T7	T8	T9	Avg
Z (mm)	15	43	75	97	120	75
Z (dia)	9.4	27.2	47.0	60.8	75.0	46.9
T_M (K)	650.0	674.2	701.4	720.3	740.0	702.1
T_S (K)	723.6	770.4	793.1	813.0	825.9	785.1
Pr	0.684	0.685	0.686	0.687	0.688	0.686
Re	16,600	16,200	15,800	15,500	15,300	15,800
Nu_{VP}	42.2	41.5	40.7	40.2	39.8	40.7
Nu_{EXP}	52.2	39.7	40.8	39.9	42.4	44.9
q_{SM} (kW/m²)	119.3	121.6	122.6	123.6	124.2	122.3

Run 613

P_M: 618 kPa T_A: 674.3 K M_A: 0.687 g/sec
T_W: 435.9 K M_W: 33.7 mg/sec

	T5	T6	T7	T8	T9	Avg
Z (mm)	15	43	75	97	120	75
Z (dia)	9.4	27.2	47.0	60.8	75.0	46.9
T_M (K)	535.0	557.8	584.5	603.4	623.0	586.5
$X_{\ell M}$ (%)	0.0	0.0	0.0	0.0	0.0	0.0
T_S (K)	436.7	590.0	676.3	704.4	719.5	630.2
Pr	0.683	0.682	0.683	0.683	0.683	0.683
Re	20,400	19,900	19,300	18,900	18,500	19,200
Nu_{VP}	49.4	48.2	47.1	46.4	45.7	47.1
Nu_{EXP}	-46.2	146.5	51.4	46.1	47.5	---
q_{SM} (kW/m²)	121.3	130.1	135.0	136.6	137.5	132.4

Run 178

P_M: 618 kPa T_A: 668.4 K M_A: 0.664 g/sec
T_W: 380.8 K M_W: 74.5 mg/sec

	T5	T6	T7	T8	T9	Avg
Z (mm)	15	43	75	97	120	75
Z (dia)	9.4	27.2	47.0	60.8	75.0	46.9
T_M (K)	394.0	416.0	440.6	458.2	477.1	442.6
$X_{\ell M}$ (%)	0.0	0.0	0.0	0.0	0.0	0.0
T_S (K)	386.5	384.8	415.9	518.8	560.4	464.5
Pr	0.692	0.689	0.687	0.686	0.685	0.687
Re	25,900	24,900	23,900	23,300	22,700	23,900
Nu_{VP}	58.3	56.8	55.2	53.9	52.8	54.9
Nu_{EXP}	-823.6	-187.8	-229.0	95.3	68.4	---
q_{SM} (kW/m²)	127.6	127.5	129.5	136.2	139.0	132.7

Run 711

P_M: 617 kPa T_A: 676.3 K M_A: 0.652 g/sec
T_W: 357.8 K M_W: 114.0 mg/sec

	T5	T6	T7	T8	T9	Avg
Z (mm)	15	43	75	97	120	75
Z (dia)	9.4	27.2	47.0	60.8	75.0	46.9
T_M (K)	372.6	374.1	375.5	376.3	377.1	375.5
$X_{\ell M}$ (%)	4.6	3.5	2.4	1.5	0.7	2.4
T_S (K)	382.8	382.1	384.2	384.5	385.2	383.4
Pr	0.694	0.694	0.693	0.693	0.693	0.693
Re	28,000	27,900	27,800	27,800	27,700	27,800
Nu_{VP}	61.5	61.4	61.3	61.2	61.1	61.3
Nu_{EXP}	662.4	843.8	775.0	829.4	835.3	---
q_{SM} (kW/m²)	135.1	135.1	135.2	135.3	135.3	135.2

Run 110

P_M: 617 kPa T_A: 467.7 K M_A: 0.654 g/sec
T_W: 346.4 K M_W: 75.6 mg/sec

	T5	T6	T7	T8	T9	Avg
Z (mm)	15	43	75	97	120	75
Z (dia)	9.4	27.2	47.0	60.8	75.0	46.9
T_M (K)	350.7	354.7	358.5	360.8	362.9	358.5
$X_{\ell M}$ (%)	6.2	5.2	4.2	3.4	2.6	4.2
T_S (K)	362.5	368.1	371.7	373.4	374.8	369.8
Pr	0.696	0.696	0.695	0.695	0.695	0.695
Re	27,800	27,600	27,400	27,300	27,100	27,400
Nu_{VP}	60.7	60.4	60.0	59.9	59.7	60.0
Nu_{EXP}	596.6	521.9	523.4	546.9	574.6	---
q_{SM} (kW/m²)	132.9	133.3	133.5	133.6	133.7	133.4

Run 910

P_M: 686 kPa T_A: 696.5 K M_A: 0.874 g/sec
T_W: N/A M_W: 0.0 mg/sec

	T5	T6	T7	T8	T9	Avg
Z (mm)	15	43	75	97	120	75
Z (dia)	9.4	27.2	47.0	60.8	75.0	46.9
T_M (K)	657.4	677.4	699.8	715.5	731.7	700.3
T_S (K)	722.4	763.7	780.7	798.2	808.8	774.4
Pr	0.684	0.685	0.686	0.687	0.688	0.686
Re	21,600	21,200	20,800	20,500	20,200	20,800
Nu_{VP}	52.5	51.7	51.0	50.4	49.9	50.9
Nu_{EXP}	63.8	47.8	50.2	48.6	51.6	54.6
q_{SM} (kW/m²)	129.6	131.9	132.9	133.9	134.5	132.6

Run 13

P_M: 687 kPa T_A: 686.3 K M_A: 0.884 g/sec
T_W: 435.5 K M_W: 45.5 mg/sec

	T5	T6	T7	T8	T9	Avg
Z (mm)	15	43	75	97	120	75
Z (dia)	9.4	27.2	47.0	60.8	75.0	46.9
T_M (K)	539.7	556.9	576.8	590.7	605.1	577.7
$X_{\ell M}$ (%)	0.0	0.0	0.0	0.0	0.0	0.0
T_S (K)	487.4	640.9	658.7	673.0	684.2	629.9
Pr	0.683	0.682	0.682	0.683	0.683	0.682
Re	26,200	25,700	25,100	24,700	24,300	25,100
Nu_{VP}	60.9	59.8	58.7	58.1	57.4	58.7
Nu_{EXP}	-84.1	54.9	55.3	54.3	55.8	---
q_{SM} (kW/m²)	118.2	127.2	128.2	129.0	129.7	126.5

Run 317

P_M: 687 kPa T_A: 687.2 K M_A: 0.918 g/sec
T_W: 354.8 K M_W: 107.2 mg/sec

	T5	T6	T7	T8	T9	Avg
Z (mm)	15	43	75	97	120	75
Z (dia)	9.4	27.2	47.0	60.8	75.0	46.9
T_M (K)	392.6	408.6	426.5	439.0	452.3	427.4
$X_{\ell M}$ (%)	0.0	0.0	0.0	0.0	0.0	0.0
T_S (K)	388.2	383.5	391.4	429.0	497.5	432.9
Pr	0.692	0.690	0.688	0.687	0.687	0.688
Re	36,000	35,000	34,000	33,300	32,600	33,900
Nu_{VP}	77.4	75.8	74.1	72.9	71.7	73.9
Nu_{EXP}	-1434.5	-239.9	-166.5	-581.3	130.7	---
q_{SM} (kW/m²)	129.9	129.6	130.1	132.9	137.8	133.1

Run 111

P_M: 686 kPa T_A: 686.4 K M_A: 0.923 g/sec
T_W: 337.5 K M_W: 152.4 mg/sec

	T5	T6	T7	T8	T9	Avg
Z (mm)	15	43	75	97	120	75
Z (dia)	9.4	27.2	47.0	60.8	75.0	46.9
T_M (K)	375.1	375.7	376.2	376.4	376.5	376.2
$X_{\ell M}$ (%)	3.9	3.1	2.3	1.7	1.1	2.3
T_S (K)	382.4	381.9	383.6	383.5	383.7	382.7
Pr	0.693	0.693	0.693	0.693	0.693	0.693
Re	39,000	39,000	39,000	39,000	39,000	39,000
Nu_{VP}	82.4	82.3	82.3	82.3	82.3	82.3
Nu_{EXP}	914.7	1067.3	900.3	942.1	923.9	---
q_{SM} (kW/m²)	133.4	133.4	133.5	133.5	133.5	133.5

Run 47

P_M: 614 kPa T_A: 343.6 K M_A: .699 g/sec
T_W: N/A M_W: 0.0 mg/sec

	T5	T6	T7	T8	T9	Avg
Z (mm)	15	43	75	97	120	75
Z (dia)	9.4	27.2	47.0	60.8	75.0	46.9
T_M (K)	353.1	377.9	405.9	425.5	445.8	407.0
T_S (K)	447.2	488.2	519.2	538.7	557.3	509.9
Pr	0.696	0.693	0.690	0.689	0.687	0.690
Re	26,600	25,300	24,000	23,200	22,500	23,900
Nu_{VP}	58.8	56.8	54.8	53.5	52.3	54.8
Nu_{EXP}	68.3	56.1	52.2	50.7	50.0	57.1
q_{SM} (kW/m²)	122.4	124.8	126.5	127.6	128.6	126.0

Run 58

P_M: 704 kPa T_A: 481.6 K M_A: 1.017 g/sec
T_W: N/A M_W: 0.0 mg/sec

	T5	T6	T7	T8	T9	Avg
Z (mm)	15	43	75	97	120	75
Z (dia)	9.4	27.2	47.0	60.8	75.0	46.9
T_M (K)	472.2	489.3	508.5	521.9	535.8	509.0
T_S (K)	539.3	571.7	591.7	606.7	619.0	585.4
Pr	0.685	0.684	0.684	0.683	0.683	0.683
Re	31,400	30,600	29,800	29,300	28,800	29,800
Nu_{VP}	70.0	68.7	67.3	66.5	65.6	67.3
Nu_{EXP}	77.1	61.9	60.0	58.1	58.3	65.1
q_{SM} (kW/m²)	125.2	127.1	128.3	129.2	129.9	127.9

Run 69

P_M: 704 kPa T_A: 480.1 K M_A: 0.982 g/sec
T_W: 336.5 K M_W: 60.1 mg/sec

	T5	T6	T7	T8	T9	Avg
Z (mm)	15	43	75	97	120	75
Z (dia)	9.4	27.2	47.0	60.8	75.0	46.9
T_M (K)	355.6	357.8	369.7	382.6	396.2	370.6
$X_{\ell M}$ (%)	0.97	0.31	0.0	0.0	0.0	0.0
T_S (K)	365.0	367.6	388.7	415.2	467.7	412.0
Pr	0.695	0.695	0.694	0.693	0.691	0.694
Re	39,400	39,200	38,300	37,300	36,400	38,200
Nu_{VP}	82.7	82.5	81.0	79.5	77.9	80.8
Nu_{EXP}	714.9	684.6	345.0	198.8	90.5	---
q_{SM} (kW/m²)	128.3	128.5	130.0	131.9	135.6	131.7

Run 78

P_M: 701 kPa T_A: 471.9 K M_A: 1.004 g/sec
T_W: 321.2 K M_W: 91.1 mg/sec

	T5	T6	T7	T8	T9	Avg
Z (mm)	15	43	75	97	120	75
Z (dia)	9.4	27.2	47.0	60.8	75.0	46.9
T_M (K)	353.1	355.5	357.7	358.9	360.1	357.6
$X_{\ell M}$ (%)	4.1	3.5	2.7	2.2	1.7	2.7
T_S (K)	360.8	365.0	367.7	368.8	369.8	366.2
Pr	0.696	0.695	0.695	0.695	0.695	0.695
Re	41,600	41,400	41,200	41,100	41,000	41,200
Nu_{VP}	86.4	86.1	85.9	85.7	85.5	85.9
Nu_{EXP}	902.2	723.9	684.2	696.3	707.4	---
q_{SM} (kW/m²)	132.0	132.3	132.5	132.6	132.7	132.4

Run 712

P_M: 662 kPa T_A: 473.4 K M_A: 1.017 g/sec
T_W: 307.0 K M_W: 182.2 mg/sec

	T5	T6	T7	T8	T9	Avg
Z (mm)	15	43	75	97	120	75
Z (dia)	9.4	27.2	47.0	60.8	75.0	46.9
T_M (K)	348.5	350.8	352.8	354.0	355.0	352.8
$X_{\ell M}$ (%)	11.8	11.2	10.6	10.1	9.6	10.6
T_S (K)	352.0	359.4	362.3	363.4	364.4	360.4
Pr	0.696	0.696	0.696	0.696	0.696	0.696
Re	46,000	45,800	45,600	45,500	45,400	45,600
Nu_{VP}	94.1	93.7	93.4	93.3	93.1	93.4
Nu_{EXP}	2021.7	818.7	743.7	746.6	748.4	---
q_{SM} (kW/m^2)	133.4	133.9	134.1	134.2	134.3	134.0

Run 118

P_M: 686 kPa T_A: 552.7 K M_A: .912 g/sec
T_W: N/A M_W: 0.0 mg/sec

	T5	T6	T7	T8	T9	Avg
Z (mm)	15	43	75	97	120	75
Z (dia)	9.4	27.2	47.0	60.8	75.0	46.9
T_M (K)	533.9	552.4	573.2	587.7	602.8	573.8
T_S (K)	599.2	633.4	652.3	668.5	680.3	646.5
Pr	0.683	0.683	0.682	0.683	0.683	0.682
Re	25,900	25,300	24,700	24,300	23,900	24,700
Nu_{VP}	60.1	59.1	58.1	57.3	56.7	58.0
Nu_{EXP}	70.6	56.3	56.5	54.7	56.3	61.3
q_{SM} (kW/m^2)	123.0	124.9	126.0	126.9	127.6	125.7

Appendix B--Determination of Heat Leaks

In this appendix the methods used for the determination of the heat leaks from the heated test section, the transition section, and the atomizer section as specified in figure 5.1 are presented.

B.1 Test Section

Losses in this section were found by conducting calibration tests with only preheated air flowing and no wall power applied. A control volume was defined along the inside surface of the tube between the centers of the inlet and outlet electrodes (INLET & OUTLET on figure 5-1). The mass flow rate of air entering and leaving was M_A. The temperatures of air at the "INLET" and "OUTLET" locations and the heat loss to ambient were to be determined.

Assuming constant fluid properties, fully developed flow, and uniform heat flux, the wall temperature varies linearly with axial location (Z) and may be expressed as:

$$T_S(Z) = T_{AI} + (4q_{SM}/GDCp)Z + q_{SM}/h \qquad B-1$$

The first two terms on the right are equivalent to the mixed-mean fluid temperature at any axial location, and the last term equivalent to the difference between the wall and mixed-mean temperatures. With no wall power applied, q_{SM} was only the loss to ambient ($q_{S\infty}$). If $q_{S\infty}$ were small, the wall and fluid

temperatures were nearly equal. This was the case for the calibration tests.

This linear model was found to closely approximate the measured wall temperature data. Accordingly, a linear relation (from a least-squares routine) was used to model measured wall temperatures, and extrapolated to the "INLET" and "OUTLET" locations. These were assumed to approximate the corresponding air temperatures, T_{AI} and T_{AO}. The test section loss was then calculated as

$$Q_{Lh} = M_A \{i_A(T_{AI}, P_I) - i_A(T_{AO}, P_O)\} \qquad B-2$$

q_{SM} (here equivalent to $-q_{S\infty}$) was assumed uniform, and calculated from Q_{Lh}. Inlet and outlet temperatures were then recalculated from equation B-1, using correlation 3-9 to determine h. The process was repeated until the solution converged.

Q_{Lh} was found for a range of wall temperatures, and was correlated against the average wall to ambient temperature difference. This resulted in an approximately constant thermal resistance defined as:

$$R_h = \{(T_{SI}+T_{SO})/2\} - T_\infty\} \; / \; Q_{Lh} \qquad B-3$$

The results of this analysis were determinations of the effective thermal resistance of the tube wall to ambient surrounds (including conduction, natural convection, and radiation effects), and inlet and outlet temperatures for specific test conditions. The thermal resistance was used in equation 5-3 to

correct the local heat flux for losses to ambient. The temperatures were used to calibrate losses in the transition and exit sections, as described below.

B.2 Transition Section

As in the heated test section, losses in the transition section were determined using calibration test results with only preheated air flowing and no test section tube wall power applied. A control volume was defined along the inside surfaces of the atomizer, transition section, and test section tube between the measuring location T3 and the center of the inlet electrode (INLET). The mass flow rate of air entering and leaving was M_A. The temperature of air leaving was T_{AI} (found as described in section B.1). The heat loss to ambient was to be determined.

With only air flowing, T3 measured the air temperature entering the transition section. Thus, the net loss to ambient was determined by

$$Q_{Lt} = M_A \{i_A(T_3,P_3) - i_A(T_{AI},P_I)\} \qquad B-4$$

where P_3 is assumed equal to the measured value P_2. The copper electrode was considered the most significant path of heat loss from this control volume. This heat leak was calucalated according to

$$Q_{LEI} = (T_{IO} - T_{II})/R_{EI}. \qquad B-5$$

using the measured values of T_{10} and T_{11}, with R_{EI} based on the assumption of one-dimensional conduction along the copper electrode. Q_{Lt} and Q_{LEI} were calculated for a number of cases and cor-related. The results indicated a proportionality.

In single-phase tests *with power input* to the test section, T_{AI} could not be determined by the method of section B.1. Further, in two-phase tests the T3 thermocouple measured not air temperature but water temperature. But Q_{LEI} could be found for these tests using B-5, so Q_{Lt} was estimated based on the proportionality:

$$Q_{Ltcurrent} = Q_{LEIcurrent} \times Q_{Ltprior}/Q_{LEIprior} \qquad B-6$$

In single-phase tests i_{AI} was calculated from B-4, while in two-phase tests 5-9 was used. This required knowledge of the atomizer loss Q_{La}.

B.3 Atomizer

For tests with only air flowing, T3 was in equilibrium with the air. Thus, the loss through the atomizer walls and insulation to ambient could be calculated directly:

$$Q_{La} = M_A \{i_A(T_{A2},P_2) - i_A(T_{A3},P_3)\}. \qquad B-7$$

From this, an overall thermal resistance (R_a) was determined as defined by:

$$Q_{La} = (T_{A2} - T_\infty)/R_a. \qquad B-8$$

C-2

Since the insulation was thick, R_a was nearly independent of M_A and T_2. Thus, a single-phase air-only test was first run to calculate R_a from B-7 and B-8. Then a two-phase test was run with minimal changes in M_A and T_2. R_a was assumed unchanged and Q_{La} calculated from B-8. This value of Q_{La} was then used in 5-9.

In two-phase tests, heat loss could also occur through the water injection tube to water flowing in it. This was estimated based on measured water temperatures and flow rates, and found to be insignificant.

1 Report No	2 Government Accession No.	3 Recipient's Catalog No
NASA CR-175076		

4 Title and Subtitle	5 Report Date
Heat Transfer to Two-Phase Air/Water Mixtures Flowing in Small Tubes With Inlet Disequilibrium	March 1986
	6 Performing Organization Code

7 Author(s)	8 Performing Organization Report No
J.M. Janssen, L.W. Florschuetz, and J.P. Fiszdon	CR-R-86001
	10 Work Unit No

9 Performing Organization Name and Address	11 Contract or Grant No
Arizona State University Dept. of Mechanical and Aerospace Engineering Tempe, Arizona 85287	NSG-3075
	13 Type of Report and Period Covered
12 Sponsoring Agency Name and Address	Contractor Report
National Aeronautics and Space Administration Washington, D.C. 20546	14 Sponsoring Agency Code
	505-69

15 Supplementary Notes

Final report. Project Manager, James W. Gauntner, NASA Lewis Research Center, Cleveland, Ohio 44135.

16 Abstract

The cooling of gas turbine components has been the subject of considerable research. The problem is difficult because the available coolant, compressor bleed air, is itself quite hot and has relatively poor thermophysical properties for a coolant. Injecting liquid water to evaporatively cool the air prior to its contact with the hot components has been proposed and studied, particularly as a method of cooling for contingency power applications. The subject of the present report is the injection of a small quantity of cold liquid water into a relatively hot coolant air stream such that evaporation of the liquid is still in process when the coolant contacts the hot component. No approach was found whereby one could confidently predict heat transfer characteristics for such a case based solely on prior studies. It was not clear whether (or to what extent) disequilibrium between phases (hot coolant air, cold liquid water) at the inlet to the hot component section would improve cooling relative to that obtained where equilibrium (i.e., complete evaporation of liquid) was established prior to contact with the hot surface. Tests were conducted with preheated air entering a small diameter electrically heated stainless steel tube. The test facility incorporated an atomizer arranged to inject a water mist into the air stream near the tube inlet. The effects of inlet disequilibrium were observed to extend downstream, first through what was interpreted as an annular-film flow regime, then through a mist flow regime, followed by a transition to single-phase in those cases for which the length of the test-section was adequate for the conditions of the test. The test results in every case showed that lower wall temperatures occurred with inlet disequilibrium. In no case was heat transfer degraded by inlet disequilibrium, either overall or locally.

17 Key Words (Suggested by Author(s))	18. Distribution Statement
Heat transfer; Gas turbine; Turbine cooling; Two-phase; Water injection; Mixture; Air-water	Unclassified - unlimited STAR Category 34

19. Security Classif. (of this report)	20 Security Classif. (of this page)	21 No of pages	22 Price*
Unclassified	Unclassified	99	A05

*For sale by the National Technical Information Service, Springfield, Virginia 22161

National Aeronautics and
Space Administration

Lewis Research Center
Cleveland, Ohio 44135

SECOND CLASS MAIL

ADDRESS CORRECTION REQUESTED

Postage and Fees Paid
National Aeronautics and
Space Administration
NASA-451

NASA